２．学会誌・雑誌等における論文掲載

掲載した論文（発表題目）	発表者氏名	発表した場所 （学会誌・雑誌等名）	発表した時期	国内・外の別
Therapy of peritoneally disseminated colon cancer by TAP-deficient ES cell-derived macrophages in allogeneic recipients.	Haga, E., Endo, Y., Haruta, M., Koba, C., Matsumura, K., Takamatsu, K., Ikeda, T., Nishimura, Y., and Senju, S.	Journal of Immunology 193: 2024-2033	2014年	国外
Application of iPS cell-derived macrophages to cancer therapy.	Senju, S., Koba, C., Haruta, M., Matsunaga, Y., Matsumura, K., Haga, E., Sasaki, Y., Ikeda, T., Takamatsu, K., and Nishimura, Y. [Author ' s view]	OncoImmunoogy 3: e27927-1-3	2014年	国外
Phase II clinical trial of multiple peptide vaccination for advanced head and neck cancer patients revealed induction of immune responses and improved OS.	Yoshitake , Y., Fukuma, D., Yuno, A. , Hirayama, M. , Nakayama, H. , Tanaka. T., Nagata, M. , Takamune, Y., Kawahara, K., Nakagawa, Y., Yoshida, R., Hirosue, A., Ogi, H., Hiraki, A. , Jono, H., Hamada, A., Yoshida, K., Nishimura, Y., Nakamura, Y., and Shinohara, M.	Clinical Cancer Research.	2014年	国外
Analysis of circulating tumor cells derived from advanced gastric cancer.	Toyoshima K, Hayashi A, Kashiwagi M, Hayashi N, Iwatsuki M, Ishimoto T, Baba Y, Baba H, Ohta Y	Int J Cancer (International Journal of Cancer)	2015年	国外
Interaction between gastric cancer stem cells and the tumor microenvironment	Ishimoto T, Sawayama H, Sugihara H, Baba H	J Gastroenterol (Journal of Gastroenterology)	2014年	国内

Ⅳ．研究成果の刊行物・別刷

THE JOURNAL OF IMMUNOLOGY

Therapy of Peritoneally Disseminated Colon Cancer by TAP-Deficient Embryonic Stem Cell–Derived Macrophages in Allogeneic Recipients

Eriko Haga, Yuko Endo, Miwa Haruta, Chihiro Koba, Keiko Matsumura, Koutaro Takamatsu, Tokunori Ikeda, Yasuharu Nishimura and Satoru Senju

J Immunol 2014; 193:2024-2033; Prepublished online 16 July 2014;
doi: 10.4049/jimmunol.1303473
http://www.jimmunol.org/content/193/4/2024

The Journal of Immunology is published twice each month by
The American Association of Immunologists, Inc.,
9650 Rockville Pike, Bethesda, MD 20814-3994.

Print ISSN: 0022-1767 Online ISSN: 1550-6606.

Therapy of Peritoneally Disseminated Colon Cancer by TAP-Deficient Embryonic Stem Cell–Derived Macrophages in Allogeneic Recipients

Eriko Haga,*,† Yuko Endo,*,† Miwa Haruta,*,† Chihiro Koba,*,† Keiko Matsumura,*,† Koutaro Takamatsu,*,† Tokunori Ikeda,*,† Yasuharu Nishimura,* and Satoru Senju*,†

We established a method to generate a large quantity of myeloid lineage cells from mouse embryonic stem (ES) cells, termed ES cell–derived proliferating myeloid cell lines (ES-ML). ES-ML continuously proliferated in the presence of M-CSF and GM-CSF. ES-ML genetically modified to express an anti-HER2 (neu) mAb single-chain V region fragment reduced the number of cocultured mouse Colon-26 cancer cells expressing HER2. Stimulation of ES-ML with IFN-γ plus LPS or TNF resulted in almost complete killing of the Colon-26 cells by the ES-ML, and the cytotoxicity was mediated, in part, by NO produced by ES-ML. When ES-ML were injected into mice with i.p. established Colon-26 tumors, they efficiently infiltrated the tumor tissues. Injection of ES-ML with rIFN-γ and LPS inhibited cancer progression in the mouse peritoneal cavity. Coinjection of TNF-transfected or untransfected ES-ML with rIFN-γ inhibited cancer growth and resulted in prolonged survival of the treated mice. In this experiment, transporter associated with Ag processing (TAP)1-deficient ES-ML exhibited therapeutic activity in MHC-mismatched allogeneic recipient mice. Despite the proliferative capacity of ES-ML, malignancy never developed from the transferred ES-ML in the recipient mice. In summary, TAP-deficient ES-ML with anticancer properties exhibited a therapeutic effect in allogeneic recipients, suggesting the possible use of TAP-deficient human-induced pluripotent stem cell–derived proliferating myeloid cell lines in cancer therapy. *The Journal of Immunology*, **2014, 193: 2024–2033.**

Macrophages reside in every tissue of the mammalian body and are engaged in various functions, such as eliminating invading pathogens, remodeling tissues, and clearing dead cells. Macrophages also infiltrate various types of cancers (1–3). Many studies indicated that tumor-associated macrophages are alternatively activated and promote cancer progression by accelerating the local invasion and metastasis of cancers (4–7). In contrast, other studies revealed the anticancer activity of macrophages in mouse or rat models (8–16). Some of these studies demonstrated the requirement for macrophages in T cell–dependent tumor rejection (11). Inoculation of TNF, PEDF, agonistic anti-CD40 mAb, CpG, or polyinosinic-polycytidylic acid into tumor-bearing mice stimulated tumor-infiltrating macrophages to kill cancer cells (12–16). These contrary observations may be due to the fact that macrophage functions are significantly affected by cytokines (17, 18).

Based on the anticancer effects of macrophages observed in preclinical studies, there have been attempts to apply macrophages to cancer therapy. For example, administration of autologous macrophages preactivated with IFN-γ to cancer patients has been tried (19–25). In the reported clinical trials, macrophages used for anticancer therapies were generated from donor peripheral blood monocytes isolated by leukapheresis. However, peripheral blood monocytes do not readily propagate; thus, the quantity, as well as the anticancer efficacy, of macrophages generated by such methods may have been insufficient to achieve therapeutic effects.

Pluripotent stem cells, such as embryonic stem (ES) cells or induced pluripotent stem (iPS) cells, can propagate indefinitely and differentiate into various types of somatic cells, including blood cells (26). Several groups, including ours, established methods to generate macrophages from mouse and human pluripotent stem cells (27–30).

In the current study, we found that introduction of the cMYC gene into mouse ES cell–derived myeloid cells (ES-MC) enabled continuous proliferation of the cells in an M-CSF– and GM-CSF–dependent manner. This procedure resulted in the generation of ES cell–derived proliferating myeloid cell lines (ES-ML), enabling us to generate a large quantity of functional macrophages. We investigated whether ES-ML with an anticancer property could exert a therapeutic effect in a mouse model of peritoneally disseminated colon cancer. In addition, we evaluated a strategy to overcome histoincompatibility between ES-ML and recipients using ES-ML deficient for transporter associated with Ag processing (TAP).

*Department of Immunogenetics, Graduate School of Medical Sciences, Kumamoto University, Kumamoto 860–8556, Japan; and †Core Research for Evolutional Science and Technology, Japan Science and Technology Agency, Kawaguchi 332–0012, Japan

Received for publication December 31, 2013. Accepted for publication June 13, 2014.

This work was supported in part by Japan Society for the Promotion of Science KAKENHI Grants 23650609, 23659158, and 24300334, Ministry of Education, Culture, Sports, Science and Technology KAKENHI Grants 22133005 and 26290057, a research grant for Intractable Diseases from the Ministry of Health and Welfare, Japan, and a grant from the Japan Science and Technology Agency.

Address correspondence and reprint requests to Dr. Satoru Senju, Department of Immunogenetics, Graduate School of Medical Sciences, Kumamoto University, Chuou-Ku, Honjo 1-1-1, Kumamoto 860-8556, Japan. E-mail address: senjusat@gpo.kumamoto-u.ac.jp

The online version of this article contains supplemental material.

Abbreviations used in this article: CBF1, (BALB/c × C57BL/6) F1; Colon/HL, HER2 and firefly luciferase–expressing Colon-26 mouse adenocarcinoma cells; ES, embryonic stem; ES-MC, ES cell–derived myeloid cell; ES-ML, ES cell–derived proliferating myeloid cell line; ES-ML/anti-HER2, ES-ML expressing an anti-HER2 single chain V region fragment; ES-ML/TNF, TNF-transfectant ES-ML; iPS, induced pluripotent stem; iPS-ML, iPS cell–derived proliferating myeloid cell line; IRES, internal ribosomal entry site; scFv, single chain V region fragment; TAP, transporter associated with Ag processing; tPA, tissue plasminogen activator.

www.jimmunol.org/cgi/doi/10.4049/jimmunol.1303473

Materials and Methods

Mice

Mouse experiments were performed under the approval of the Animal Research Committee of Kumamoto University. Six- to eight-wk-old BALB/c or (BALB/c × C57BL/6) F1 (CBF1) mice were purchased from Japan SLC (Hamamatsu, Japan) and housed under specific pathogen–free conditions at the Center for Animal Resources and Development (Kumamoto University).

Flow cytometric analysis

The following mAb conjugated with FITC or PE were purchased from BD Pharmingen (San Diego, CA), Miltenyi Biotec (Bergisch Gladbach, Germany), or eBioscience (San Diego, CA): anti-CD45 (clone 30-F11), anti-CD11b (clone M1/70), anti-CD14 (clone Sa2-8), anti-F4/80 (clone BM8), anti-HER2/neu (clone Neu 24.7), anti-cMYC (clone SH1-26E7.1.3.), and anti–H2-K^b (AF6-88.5.5.3). Polyclonal goat anti-mouse TNFRI and II Ab, polyclonal goat IgG (R&D Systems, Minneapolis, MN), and FITC-conjugated rabbit anti-goat IgG Ab (Sigma-Aldrich, St. Louis, MO) also were used. Cells were stained with the fluorochrome-conjugated mAb for 40 min and then washed twice with PBS containing 2% FCS. Stained cells were analyzed on a FACScan or FACSCalibur flow cytometer (Becton Dickinson).

Generation of ES-ML

ES cells derived from the C57BL/6 strain were kindly provided by Drs. N. Nakatsuji and H. Suemori (Kyoto University, Kyoto, Japan). Gene targeting of the TAP1 gene in E14 ES cells derived from the 129/sv strain (H-2^b) to generate TAP$1^{-/-}$ ES cells was performed as reported previously (31). Differentiation of ES cells to generate ES-MC was performed as described previously (32). The human cMYC gene was introduced into ES-MC, prepared from the second step of the differentiation culture, using a lentiviral vector to establish a proliferating myeloid cell line (ES-ML). ES-ML were maintained in RPMI 1640 medium containing 10% FCS, mouse GM-CSF (10–20 ng/ml), and human M-CSF (20–50 ng/ml).

Construction of HER2 and anti-HER2 mAb expression vectors

cDNA for mAb single chain V region fragment (scFv) specific to HER2 (neu) was a gift from Dr. J. Lieberman (Addgene plasmid #10794, Harvard Medical School, Boston, MA) (33). The scFv sequence was linked by PCR with DNA encoding a cMYC tag (EQKLISEEDL) and a C-terminal

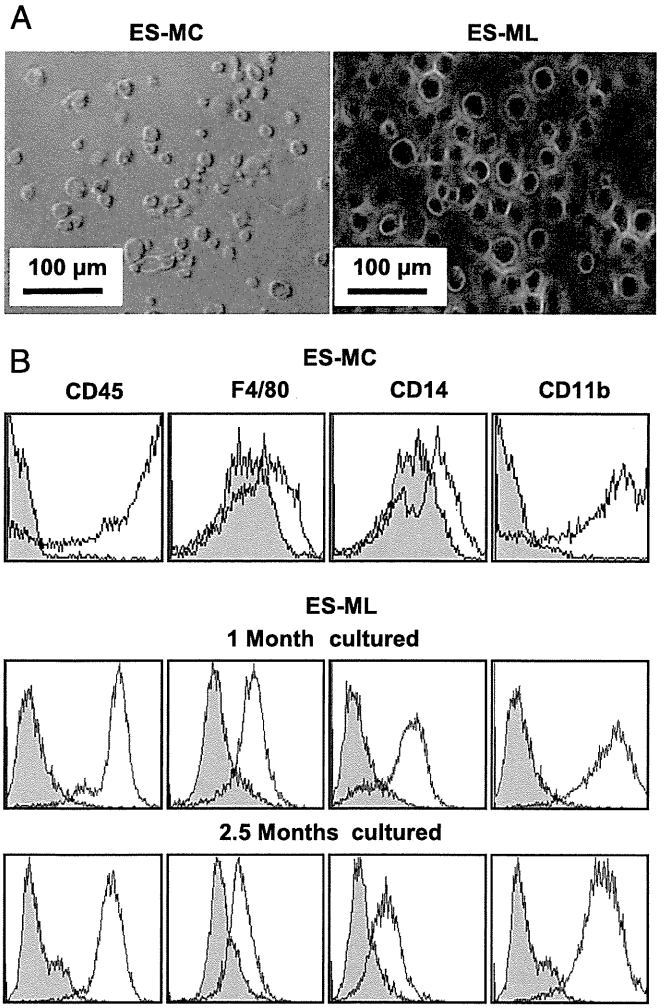

FIGURE 1. Characterization of 129 mouse ES-ML. (**A**) Phase-contrast images of ES-MC and ES-ML. (**B**) Flow cytometric analysis of CD45, CD11b, F4/80, and CD14 on ES-MC and ES-ML. ES-MC were generated by differentiation culture established previously (32). ES-ML cultured for 1 or 2.5 mo after introduction of c-Myc were analyzed. The staining profiles of specific mAbs (open graph) and isotype-matched control mAbs (shaded graph) are shown.

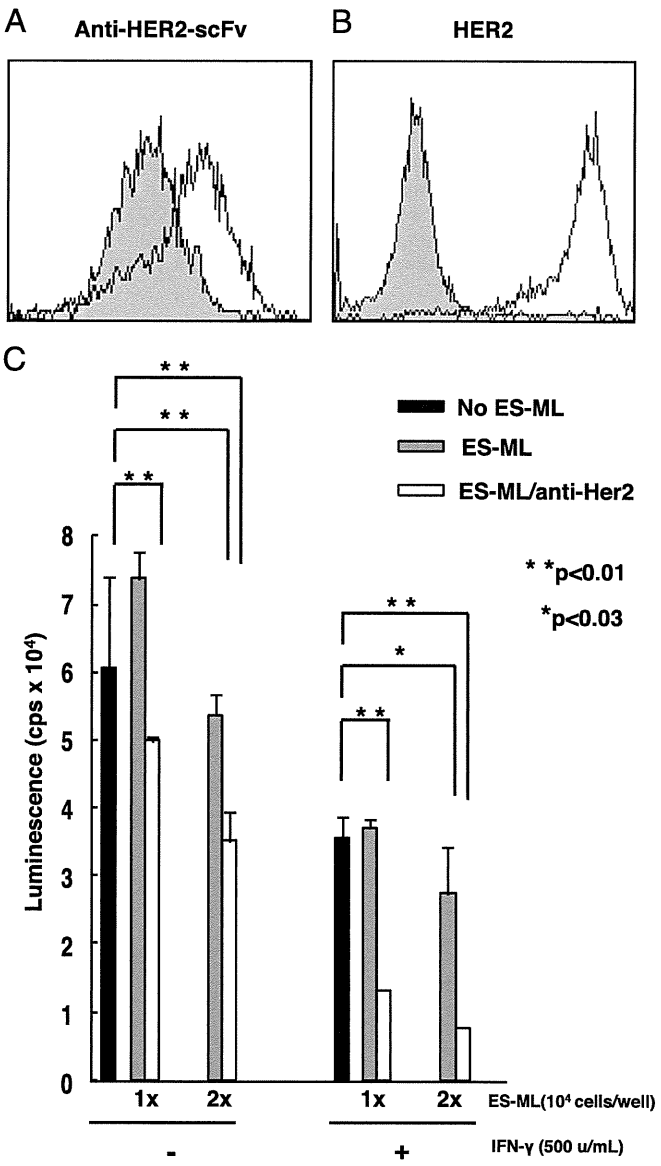

FIGURE 2. Anticancer effect of ES-ML/anti-HER2. (**A**) Expression of an anti-HER2 scFv in ES-ML/anti-HER2 was analyzed by staining with an anti-cMYC tag mAb. The staining profiles of the anti-cMYC tag mAb (open graph) and isotype-matched control mAb (shaded graph) are shown. (**B**) Expression of HER2 in HER2 and firefly luciferase–expressing Colon-26 mouse adenocarcinoma cells (Colon/HL). (**C**) Colon/HL (5×10^3 cells/well) were cultured alone (black bars) or cocultured with 1 or 2×10^4 ES-ML (gray bars) or ES-ML/anti-HER2 (white bars) in the presence or absence of IFN-γ (500 U/ml) in a 96-well culture plate. After 3 d of culture, the number of live Colon/HL was measured by luciferase activity. Data are mean luminescence counts per second (cps) + SD of duplicate assays.

fragment of mouse FcγRI. cDNA for HER2 was obtained from the human breast cancer cell line MCF7. The cDNA were cloned into the mammalian expression vector pCAG- internal ribosomal entry site (IRES)-puroR driven by the CAG promoter and including an IRES-puromycin *N*-acetyltransferase gene cassette.

Generation of lentiviral vectors

cDNA of human cMYC and mouse TNF were obtained by PCR and cloned into a pENTR-TOPO vector (Invitrogen, Carlsbad, CA). The cDNA fragments were inserted into the lentiviral vector CSII-EF (34) (a gift from Dr. H. Miyoshi together with the packaging constructs, RIKEN, Tsukuba, Japan), with or without IRES-puroR, to generate lentiviral expression constructs. Recombinant lentivirus was produced and purified by a previously described method (28).

Analysis of the antitumor activity of ES-ML in vitro

Colon-26 mouse adenocarcinoma cells, provided by RIKEN, were transfected with expression vectors for HER2 and firefly luciferase by electroporation to generate HER2 and firefly luciferase–expressing Colon-26 mouse adenocarcinoma cells (Colon/HL). Colon/HL ($2.5–5 \times 10^3$ cells/well) were cultured with the indicated numbers of ES-ML in the presence of IFN-γ (PeproTech, Rocky Hill, NJ), LPS (Sigma-Aldrich), mouse TNF (PeproTech), L-NAME (Dojindo, Kumamoto, Japan), L-NMMA (Dojindo), or NOR-5 (Dojindo) in 96-well flat-bottom culture plates (B&W Isoplate; PerkinElmer, Waltham, MA). After 3 d of culture, 50 μl luciferase substrate solution (steadylite plus; PerkinElmer) was added to each well, and the luminescence was measured by a microplate reader (TriStar; Berthold Technologies, Bad Wildbad, Germany). In some experiments, ES-ML were pretreated with IFN-γ (200 U/ml), IFN-γ plus LPS (0.03 μg/ml), or IFN-γ plus TNF (10 ng/ml) for 24 h, harvested, and washed. The pretreated or untreated ES-ML (1×10^4 cells/well) were cocultured with Colon/HL (2.5×10^3 cells/well). Production of NO in ES-ML was quantified by determining the concentration of $NO_2 + NO_3$ in culture supernatants by the Griess method using a NO assay kit (Dojindo).

Analysis of ES-ML cell infiltration into cancer tissues

Colon-26 cells (2×10^6 cells/mouse) were injected into the peritoneal cavity of BALB/c mice. After 7 d, ES-ML labeled with PKH26 (Sigma-Aldrich) were injected i.p. into the mice (5×10^7 cells/mouse), with or without tissue plasminogen activator (tPA; 5000 U/mouse; Technoclone, Vienna, Austria). Mice were sacrificed on the next day, and cancer tissues in the greater omentum and mesenterium were removed, fixed in 4% paraformaldehyde/PBS, and embedded in Tissue-TEK O.C.T. compound (Sakura Finetek, Tokyo, Japan). Twenty-micron-thick frozen sections were prepared on a cryostat (MICROM HN505N; Thermo Scientific, Kalamazoo, MI), nuclear stained with DAPI, and analyzed under a fluorescence microscope (Axio Observer Z1; Carl Zeiss, Oberkochen, Germany).

Analysis of the antitumor activity of ES-ML in vivo

Mice were injected i.p. with Colon/HL ($1–2 \times 10^6$ cells/mouse). On day 2, D-Luciferin (3 mg/mouse; Advanced Assay Technologies, Sunnyvale, CA) was injected i.p. into the anesthetized mice, and luminescence images

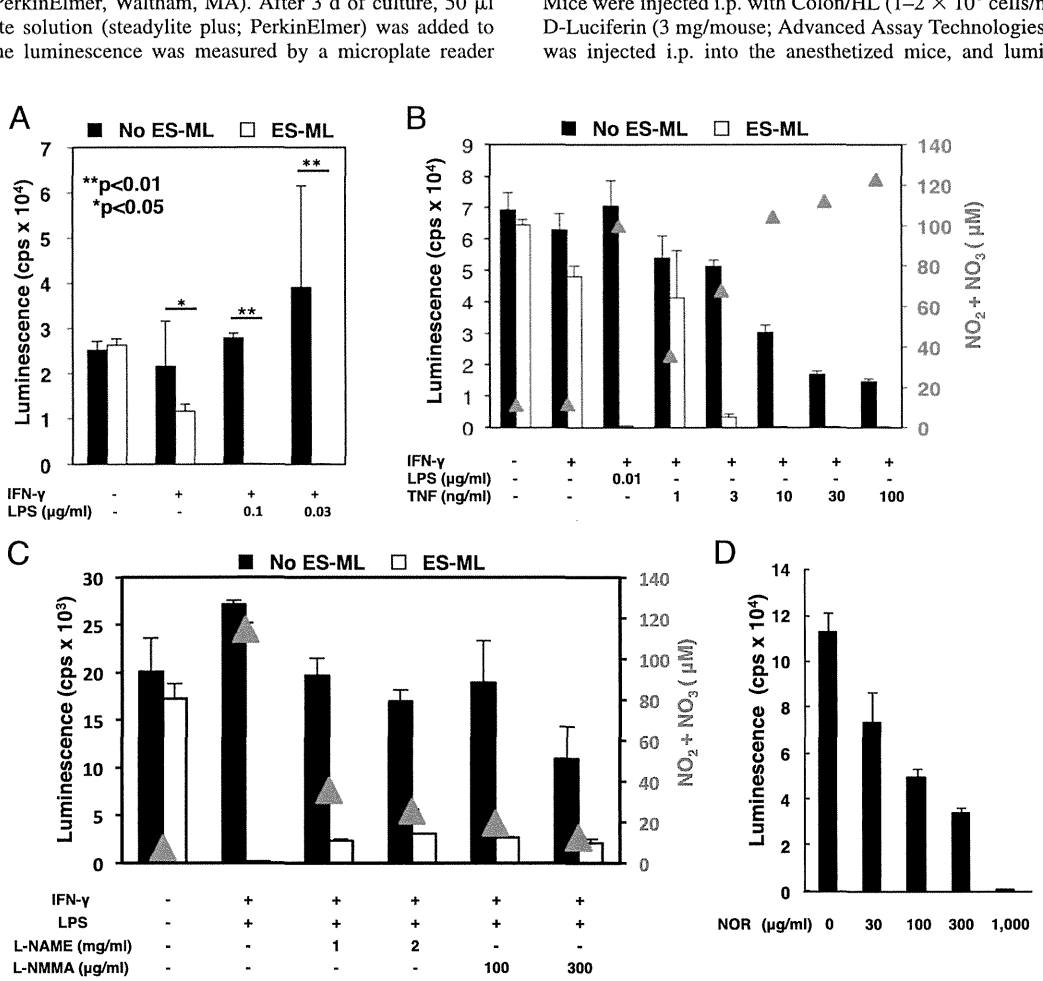

FIGURE 3. Anticancer effect of ES-ML stimulated with IFN-γ plus LPS or TNF. (**A**) Colon/HL (2.5×10^3 cells/well) were cultured alone (black bars) or cocultured with ES-ML/anti-HER2 (1×10^4 cells/well; white bars) in a 96-well culture plate in the presence or absence of IFN-γ (200 U/ml) and LPS (0.1 or 0.03 μg/ml). The number of live Colon/HL was measured on day 3 by luciferase activity. (**B**) Colon/HL (2.5×10^3 cells/well) were cultured alone (black bars) or cocultured with ES-ML/anti-HER2 (1×10^4 cells/well; white bars) in the presence or absence of IFN-γ (200 U/ml), LPS (0.01 μg/ml), or TNF (1–100 ng/ml) for 3 d. NO production from ES-ML was measured by quantifying the concentrations of NO_2 and NO_3 in the culture supernatant by the Griess method; the results are indicated by red triangles. (**C**) Colon/HL (2.5×10^3 cells/well) were cultured alone (black bars) or cocultured with ES-ML/anti-HER2 cells (white bars) in a 96-well culture plate in the presence or absence of IFN-γ (200 U/ml), LPS (0.1 μg/ml), L-NAME (1 or 2 mg/ml), or L-NMMA (100 or 300 μg/ml) for 3 d. Production of NO by ES-ML was measured and presented as in (B). The number of live Colon/HL was determined by luciferase activity. (**D**) Colon/HL (2.5×10^3 cells/well) were cultured in a 96-well culture plate in the presence or absence of NOR-5 (30–1000 μg/ml) for 24 h. The number of live Colon/HL was determined by luciferase activity. Data are the mean luminescence counts per second (cps) + SD of triplicate (A, B, and D) or duplicate (C) assays.

were obtained by an in vivo imaging system (NightOWL II; Berthold Technologies) under anesthesia with isoflurane inhalation plus tribromoethanol injection. Mice carrying established tumors were divided into therapy and control groups. Therapy group mice were administered ES-ML and IFN-γ. In some experiments, LPS, M-CSF, collagenase, and hyaluronidase also were administered, as indicated. Cancer progression was monitored by luminescence imaging analysis on days 7 and 14 and quantified by the total luminescence count for each mouse.

Statistical analysis

Student t test was used for the statistical analysis of data from in vitro experiments. Statistical analysis of the results from in vivo experiments was done using the Mann–Whitney U test or the log-rank test, as indicated. A p value < 0.05 was considered significant.

Results

Generation and characterization of mouse ES-MC with a proliferative capacity

We previously established a method to generate dendritic cells and macrophages from mouse pluripotent stem cells (23, 28). In the current study, we found that forced expression of cMYC induced proliferation of ES-MC and established the method to generate ES-ML (Fig. 1A). Both ES-MC and ES-ML expressed the panleukocyte marker CD45 and macrophage markers F4/80, CD14, and CD11b (Fig. 1B). ES-ML continuously grew in the presence of GM-CSF and M-CSF for at least several months, with a doubling time of 2–3 d. This simple technique enabled us to readily generate a large quantity of mouse myeloid cells.

Anticancer effect of ES-ML in vitro

HER2/neu is expressed in various human malignancies, including colon cancer (35, 36). A humanized Ab against HER2, trastuzumab, is widely used for the treatment of breast and gastric cancers (37, 38). Ab-dependent cellular cytotoxicity mediated by NK cells and macrophages is considered a critical mechanism underlying the effect of anticancer Ab therapies (39). We expected that ES-ML expressing an anti-HER2 scFv (ES-ML/anti-HER2) would attack cancer cells expressing HER2. To ensure that the transfectant ES-ML execute Ab-dependent cellular cytotoxicity mimicking cytotoxicity upon encounter with HER2-expressing target cells, the scFv was linked to the transmembrane and cytoplasmic domains of FcγRI. Cell surface expression of scFv fused to FcγRI was detected by staining with anti-cMYC tag mAb (Fig. 2A).

We evaluated the effect of ES-ML/anti-HER2 against cancer cells expressing HER2 in vitro. To this end, we generated Colon/HL (Fig. 2B). We established an experimental system to examine the effect of ES-ML on cocultured Colon/HL, in which the number of live Colon/HL was quantitated by luciferase activity. ES-ML/anti-HER2 showed a certain degree of activity to reduce the number of cocultured Colon/HL (Fig. 2C). Addition of IFN-γ to the culture synergistically enhanced the effect of ES-ML/anti-HER2 on Colon/HL (Fig. 2C).

We tested several factors for their ability to enhance the anticancer effect of ES-ML and found that simultaneous addition of IFN-γ plus LPS resulted in almost complete killing of Colon/HL (Fig. 3A). The disappearance of live Colon/HL induced by IFN-γ plus LPS was observed only in the presence of ES-ML (Fig. 3A). Therefore, the dramatic killing of Colon/HL was not a direct effect of IFN-γ and LPS on Colon/HL but was mediated by ES-ML stimulated with IFN-γ plus LPS. The dramatic killing of Colon/HL by ES-ML also was observed when IFN-γ plus TNF were added to the coculture (Fig. 3B). In contrast, ES-ML pretreated with IFN-γ, IFN-γ plus LPS, or IFN-γ plus TNF for 24 h did not exhibit significant killing of Colon/HL, suggesting that the anticancer effect of ES-ML induced by the factors promptly decreased after removal of the stimulating factors (Supplemental Fig. 1).

Induction of NO synthase 2 and production of NO by mouse macrophages upon stimulation with IFN-γ and LPS were reported previously (40, 41). ES-ML also produced NO when stimulated with IFN-γ plus LPS or IFN-γ plus TNF, and the magnitude of cytotoxicity was in parallel with the amount of NO produced by ES-ML (Fig. 3B). To assess the possibility that the killing of Colon/HL was mediated by NO, we added NO synthase inhibitors, L-NAME or L-NMMA (42), to the cultures. Colon/HL cell death was partly inhibited by either of these drugs (Fig. 3C), suggesting that the cytotoxicity was mediated by NO, at least in part. In addition, a NO-donor chemical (NOR-5) killed Colon/HL in

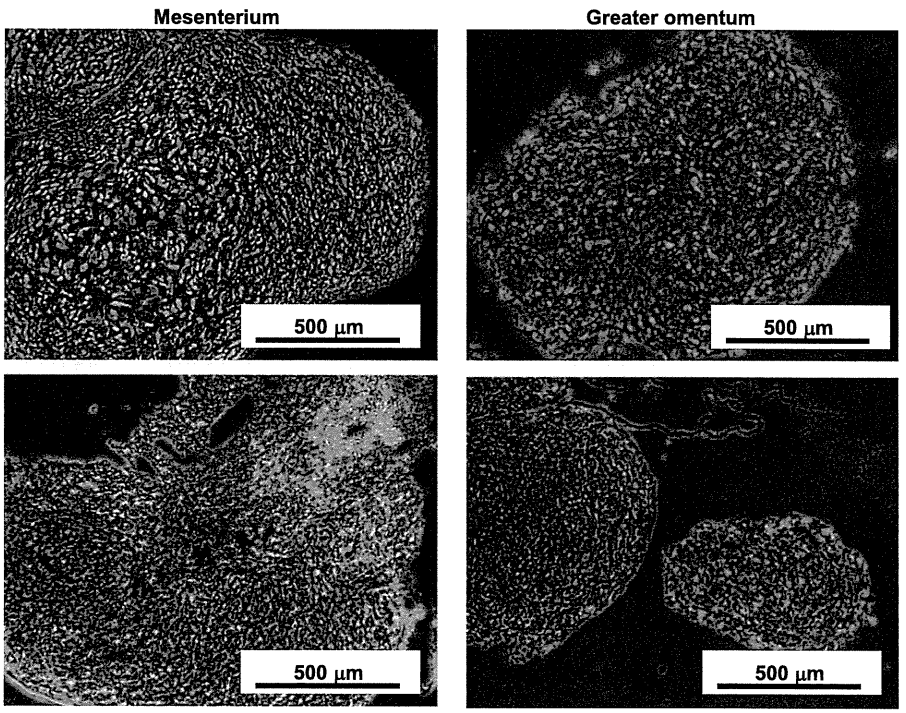

FIGURE 4. Infiltration of i.p. injected ES-ML into tumor tissues. Colon/HL (2×10^6 cells/mouse) were injected into the peritoneal cavity of mice. After 7 d, ES-ML labeled with the fluorescent dye PKH26 were injected i.p. into the mice (5×10^7 cells/mouse) with (*lower panels*) or without (*upper panels*) tPA (5000 U/mouse). The mice were sacrificed the next day, and the tumor tissues in the peritoneal cavity were isolated, fixed, and sectioned at 20-μm thicknesses. The sections were stained with DAPI and analyzed under a fluorescence microscope. Cancer tissues isolated from the mesenterium and greater omentum are shown. PKH26–labeled ES-ML were visualized by red fluorescence.

a dose-dependent manner (Fig. 3D), indicating that Colon/HL is sensitive to NO.

Infiltration of ES-ML into cancer tissues in vivo

Macrophage infiltration is frequently observed in clinical samples of cancer tissues. We examined whether exogenously administered ES-ML also infiltrated pre-established cancer tissues in vivo. We injected Colon/HL i.p. into the mice. After 7 d, we injected ES-ML labeled with the fluorescent dye PKH26. For some mice, we injected tPA simultaneously with ES-ML, intending to enhance the tissue infiltration of ES-ML. The next day, the mice were sacrificed, and the tumor masses in the greater omentum and mesenterium were collected for microscopic examination.

Fig. 4 shows the fluorescence images of the tumor tissue sections. We observed infiltrating ES-ML in the cancer tissues, indicating migration of ES-ML directed to tumor tissues. Coinjection with tPA seemed to enhance the infiltration of ES-ML into cancer tissues.

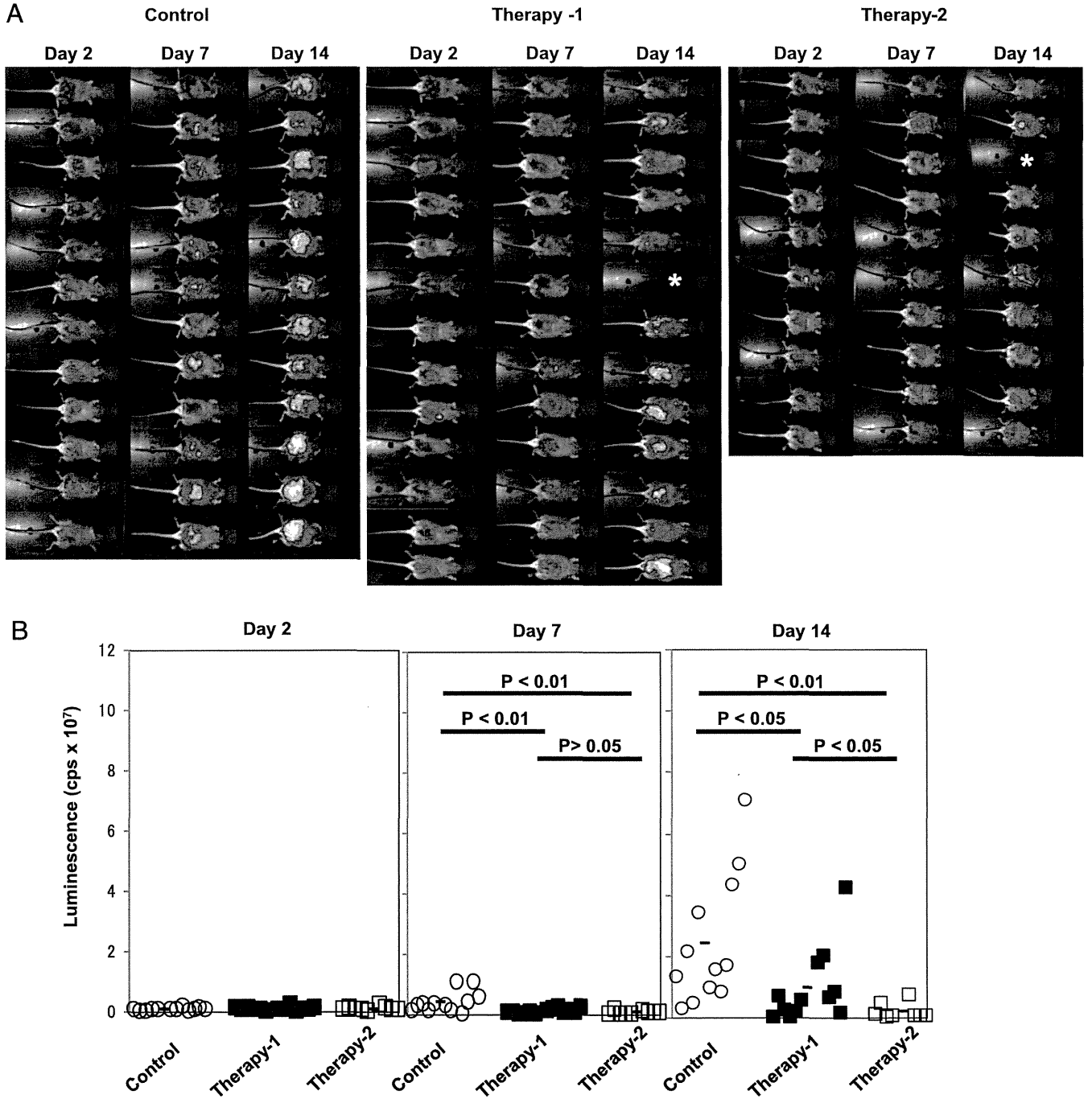

FIGURE 5. Therapeutic effect of coinjection of ES-ML along with IFN-γ plus LPS on peritoneally disseminated cancer. Colon/HL were injected i.p. into CBF1 mice (1×10^6 cells/mouse). On day 2, the mice were subjected to luminescence imaging analysis (**A**) and divided into control [○ in (**B**); $n = 12$], therapy-1 (■; $n = 13$), and therapy-2 (□; $n = 10$) groups. Mice in therapy-1 and -2 groups were injected i.p. with IFN-γ (2×10^4 U) and LPS (1 μg) on days 3, 5, 8, 10, and 12. In addition, mice in therapy-2 group were injected i.p. with ES-ML/anti-HER2 cells (5×10^7), collagenase (20 μg), hyaluronidase (600 μg), and M-CSF (1 μg) on days 2, 4, 7, 9, and 11. To follow the tumor growth, all mice were subjected to bioluminescence analysis on days 7 and 14. (B) Total luminescence signals of individual mice were plotted. One mouse in the therapy-1 group and one mouse in the therapy-2 group died between days 7 and 14 [indicated by asterisks in (A)]. The statistical differences in the values between mouse groups on days 7 and 14 were analyzed using the Mann–Whitney *U* test.

Therapeutic effect of ES-ML with IFN-γ plus LPS on peritoneally disseminated cancer

Based on the cytotoxic effect on Colon/HL by ES-ML stimulated with IFN-γ plus LPS in vitro and the infiltration of exogenously administered ES-ML into cancer tissues in vivo, we expected that administration of ES-ML with IFN-γ plus LPS would exert a therapeutic effect against cancer in vivo.

Colon-26 cells, the parental cells of Colon/HL, were derived from the BALB/c (H-2^d) mouse strain, and the ES-ML used in this study were derived from ES cells of C57BL/6 origin. To avoid immune-mediated rejection of the transferred cancer and ES-ML, we used CBF1 mice as recipients. We injected Colon/HL i.p. into CBF1 mice. After 2 d, we examined the establishment of cancer in the mouse peritoneal cavity by bioluminescence analysis. Mice with established Colon/HL cancer were divided into a control group and two therapy groups. The mice in therapy-1 and -2 groups were injected i.p. with LPS plus IFN-γ three times/week. In addition, mice in therapy-2 group were injected with ES-ML/anti-HER2 cells plus collagenase, hyaluronidase, and M-CSF. Mice in the control group were left untreated. The growth of tumors was monitored by bioluminescence analysis on days 7 and 14. The results of imaging analysis are shown in Fig. 5A, and luminescence counts of individual mice are represented by the dot plots in Fig. 5B.

Cancer growth in the mice in therapy-1 group was significantly inhibited compared with the control group ($p < 0.05$). The cancer-inhibitory effect observed in mice in therapy-1 group may have been exerted by endogenous macrophages stimulated by the administered LPS and IFN-γ. One mouse in the therapy-1 group died between days 7 and 14, probably because of the toxic effect of LPS. Cancer growth in the therapy-2 group was retarded more dramatically than in the therapy-1 group ($p < 0.05$) and the control group ($p < 0.01$), indicating that exogenously transferred ES-ML exerted an anticancer effect. However, one mouse in therapy-2 group also died between days 7 and 14.

Anticancer effect of ES-ML expressing TNF with rIFN-γ

As described above, some of the mice administered LPS plus IFN-γ, with or without ES-ML, died before day 14, probably due to the toxicity of the injected LPS. As shown in Fig. 3B, ES-ML killed Colon/HL in the presence of IFN-γ plus LPS, as well as in the presence of IFN-γ plus TNF. We considered that transfer of ES-ML genetically modified to produce TNF must be less toxic for the mice than injection of LPS or rTNF, because production of TNF by the cancer tissue–infiltrating transfectant ES-ML resulted in more local action of TNF and a lower systemic effect.

We successfully generated transfectant ES-ML producing TNF by lentivirus-mediated transduction (Fig. 6A). Next, we analyzed

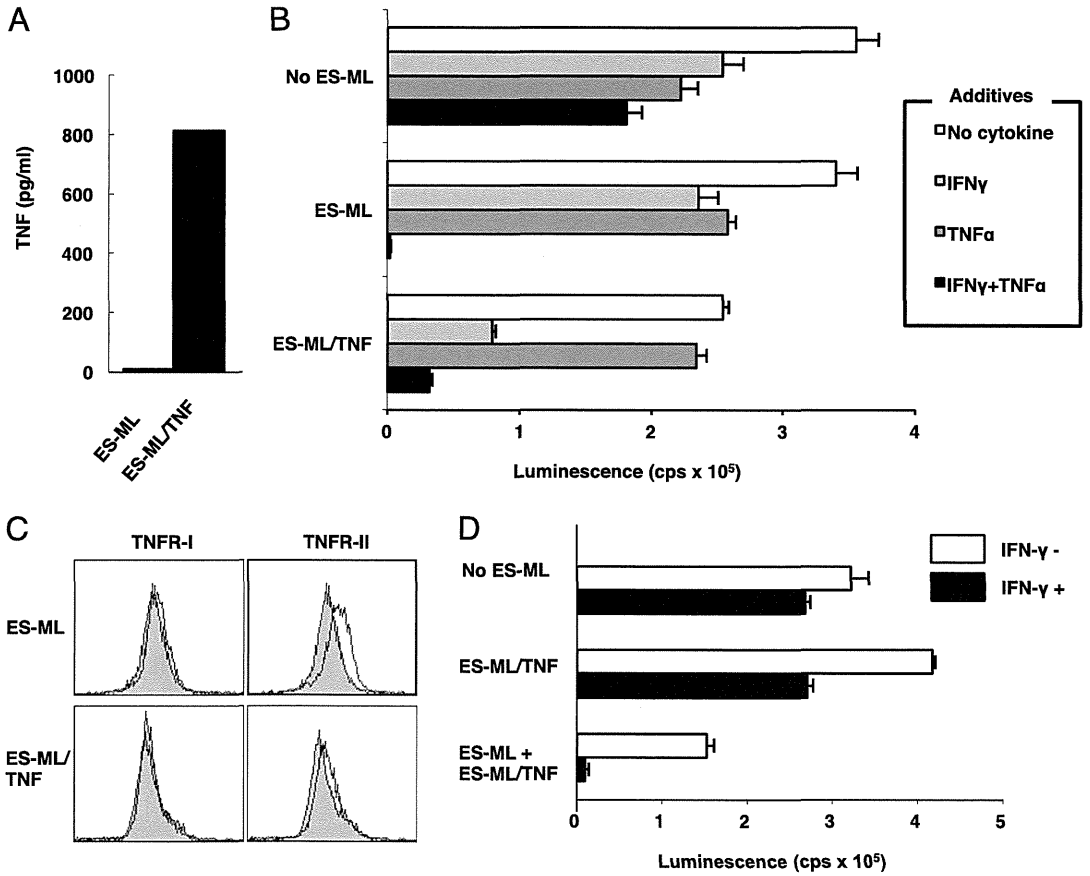

FIGURE 6. Cytotoxicity of ES-ML, with and without production of TNF, against Colon/HL in the presence of IFN-γ. (**A**) ES-ML, with or without TNF transgene, were cultured in a 96-well culture plate (1×10^4 cells/100 μl/well). After 24 h, the culture supernatants were collected, and the concentration of TNF was measured by ELISA. (**B**) Colon/HL (2.5×10^3 cells/well) were cultured alone or cocultured with untransfected ES-ML (1×10^4 cells/well) or ES-ML/TNF (1×10^4 cells/well) in a 96-well culture plate in the absence of cytokine or the presence of IFN-γ (200 U/ml), TNF (10 ng/ml), or IFN-γ plus TNF. The number of live Colon/HL was measured by luciferase activity after 3 d of culture. Data are the mean + SD of triplicate assays. (**C**) Flow cytometric analysis of TNFR-I and -II expression in ES-ML and ES-ML/TNF. The staining profiles of the specific mAb (open graphs) and isotype-matched control mAb (shaded graphs) are shown. (**D**) Colon/HL (2.5×10^3/well) were cultured alone or cocultured with ES-ML/TNF (1×10^4 cells/well) or a combination of ES-ML/TNF (5×10^3 cells/well) and ES-ML (5×10^3 cells/well) in the absence or presence of IFN-γ (200 U/well). The number of live Colon/HL was measured by luciferase activity after 3 d of culture. Data are the mean ± SD of triplicate assays.

the in vitro effect of TNF-transfectant ES-ML (ES-ML/TNF) on Colon/HL in the presence of rIFN-γ. Contrary to our expectation, ES-ML/TNF with rIFN-γ were not as effective as ES-ML with rIFN-γ plus rTNF (Fig. 6B). ES-ML/TNF also were less effective than ES-ML in the presence of rIFN-γ plus rTNF (black bars in Fig. 6B), suggesting that the reactivity of ES-ML/TNF to TNF was lower than that of nontransfected ES-ML. Indeed, expression of TNFR-I and -II in ES-ML/TNF was decreased compared with that in nontransfected ES-ML (Fig. 6C). Probably, cells with lower TNF sensitivity selectively survived during the establishment of ES-ML/TNF. Consistent with these results, in the presence of IFN-γ, the combination of ES-ML/TNF with untransfected ES-ML exhibited more potent cytotoxicity against Colon/HL than did ES-ML/TNF only (Fig. 6D).

Anticancer effect of TAP1-deficient ES-ML in allogeneic mice

We next examined the anticancer effect of ES-ML/TNF in vivo. Because the reactivity of ES-ML/TNF to TNF was impaired, as described above, we simultaneously injected ES-ML/TNF and untransfected ES-ML with rIFN-γ. In these experiments, we used BALB/c mice with an H-2^d MHC haplotype as recipient mice. For the treatments, we used ES-ML derived from TAP1-deficient E14 ES cells (31). Although E14 ES cells originated from the 129/sv strain with an H-2^b MHC haplotype, cell surface expression

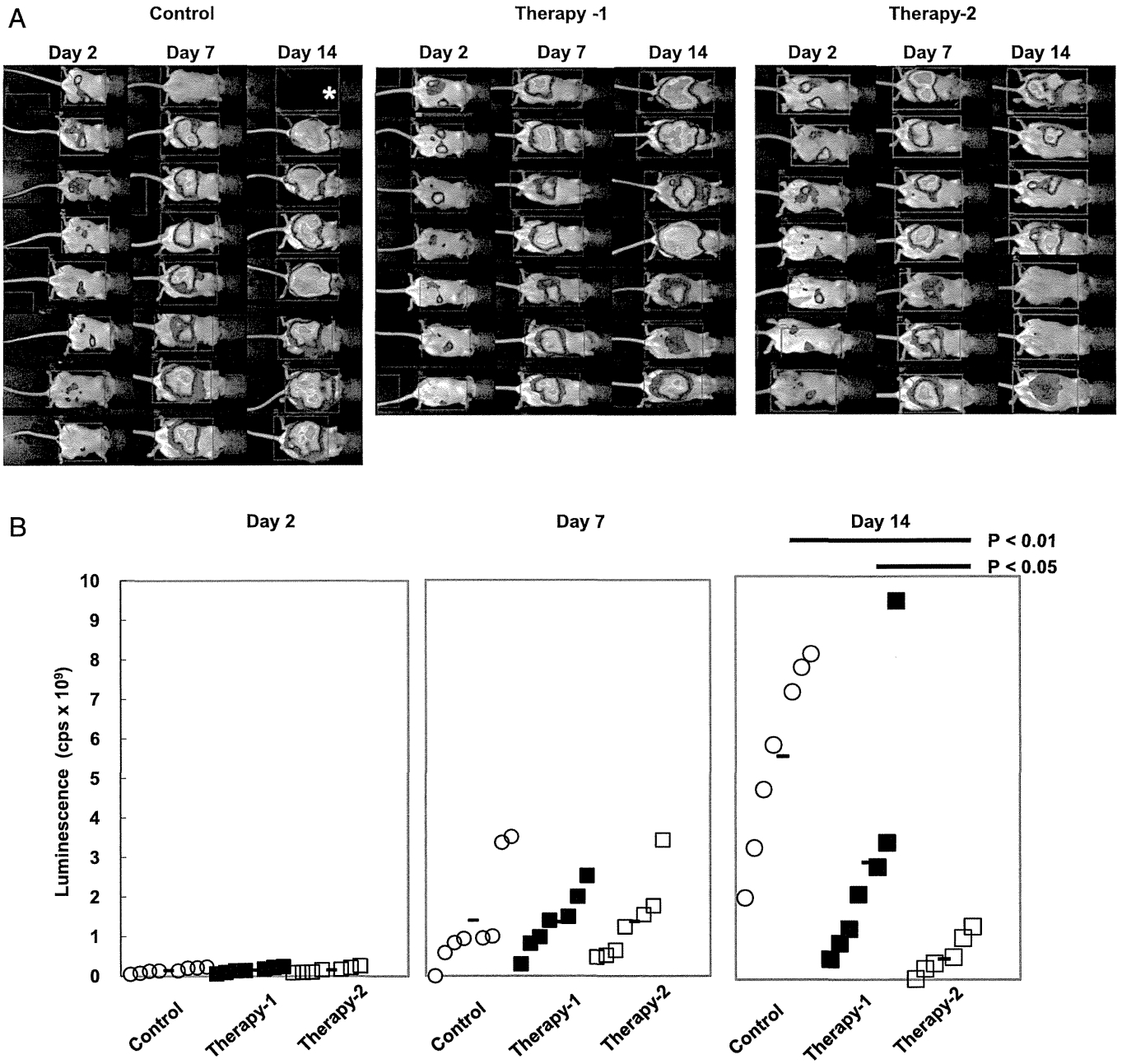

FIGURE 7. Therapeutic effect of TAP1-deficient ES-ML in cancer-bearing allogeneic mice. Colon/HL were injected i.p. into BALB/c mice (2×10^6 cells/mouse). On day 2, the mice were subjected to luminescence imaging analysis (**A**) and divided into control [○ in (**B**), $n = 8$], therapy-1 (■, $n = 7$), and therapy-2 (□, $n = 7$) groups. Mice in therapy-1 group were injected i.p. with IFN-γ (1×10^4 U) twice a week from day 3. Mice in therapy-2 group were injected i.p. with IFN-γ (1×10^4 U) along with TAP1$^{-/-}$ ES-ML ($1–3 \times 10^7$) and TAP1$^{-/-}$ ES-ML/TNF ($1–3 \times 10^7$) twice a week from day 3. To follow the tumor growth, all mice were subjected to bioluminescence analysis on days 7 and 14. (B) Total luminescence signals of individual mice were plotted. One mouse in the control group died between days 7 and 14 [indicated by an asterisk in (A)]. The statistical differences in the value between mouse groups on day 14 were analyzed by the Mann–Whitney *U* test.

of MHC class I was almost completely diminished in TAP1-deficient ES-ML (Supplemental Fig. 2). We expected that, upon injection into BALB/c mice, TAP1-deficient ES-ML could avoid attack by allogeneic MHC class I–reactive CTL, the major effectors in the acute rejection of allogeneic cells, and exert an anticancer effect.

We injected Colon/HL (H-2^d) into BALB/c mice (H-2^d). After 2 d, we examined the establishment of cancer in the mouse peritoneal cavity by bioluminescence analysis. Mice with established Colon/HL cancer were divided into an untreated (control) group and two treatment (therapy-1 and therapy-2) groups. The mice in therapy-1 group were treated with IFN-γ only. Mice in therapy-2 group were treated with ES-ML plus ES-ML/TNF, both TAP1-deficient, along with rIFN-γ. As shown in Fig. 7A and Fig. 7B, cancer progression was significantly inhibited in mice of therapy-2 group compared with those in therapy-1 group ($p < 0.05$) and the control group ($p < 0.01$). Moreover, survival of therapy-2 group mice was significantly extended compared with therapy-1 group and control group mice ($p < 0.01$, Fig. 8).

To investigate malignancy development from TAP-deficient ES-ML in the allogeneic recipients, we injected TAP-deficient ES-ML into BALB/c mice without tumor cell inoculation and observed them for up to 12 wk. During the observation period, mice were completely healthy, and no significant difference in body weight was observed between ES-ML–injected mice and control mice without ES-ML injection (Supplemental Fig. 3). Eight or twelve weeks after the ES-ML injection, the mice were sacrificed, dissected, and examined carefully under a stereomicroscope. We found no difference between ES-ML–inoculated mice and control mice, concluding that no malignancy developed from ES-ML.

These results indicate that, when administered into allogeneic cancer-bearing mice, TAP-deficient ES-ML can overcome the barrier of histoincompatibility and produce a therapeutic effect. Despite the proliferative capacity of ES-ML, TAP-deficient ES-ML did not cause malignancy in the allogeneic recipient mice, indicating that ES-ML therapy is safe in terms of cancer risk.

Discussion

In the current study, we developed a method to generate a large quantity of myeloid cells from mouse ES cells. The myeloid cells with a proliferative capacity, termed ES-ML, exhibited macrophage-like morphology and cell surface markers. ES-ML/anti-HER2 caused a reduction in the number of HER2-expressing Colon-26 cancer cells in coculture experiments. This anticancer effect of ES-ML/anti-HER2 was enhanced by addition of IFN-γ. A more dramatic anti-Colon-26 effect of ES-ML was observed when it was added with IFN-γ plus LPS or IFN-γ plus TNF, resulting in almost complete disappearance of cocultured Colon-26. Although it was suggested that this anticancer effect was mediated, in part, by NO produced by ES-ML, other mechanisms are likely involved. For example, production of molecules with cytotoxic effects, such as reactive oxygen species, proteases, Fas-ligand, TRAIL, and type I IFNs, is a possible mechanism. In addition, phagocytic killing may be involved in the tumor-suppressive effect of macrophages, as we (28) and other investigators (43) previously observed. Exogenously inoculated ES-ML efficiently infiltrated the cancer tissues in mice. Administration of ES-ML with IFN-γ plus LPS inhibited the growth of pre-established Colon/HL cancer in the peritoneal cavity of the mice.

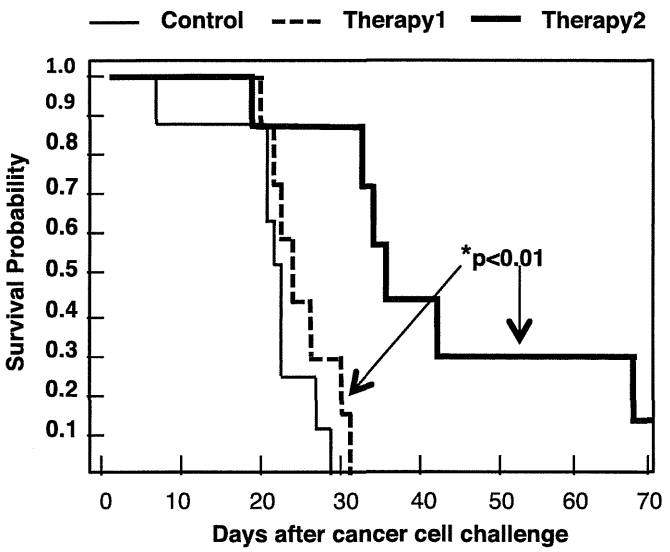

FIGURE 8. Survival of cancer-inoculated mice. Survival curves of control, therapy-1, and therapy-2 mouse groups. The differences between therapy-2 and control groups, as well as between therapy-2 and therapy-1 groups, were statistically significant (log-rank test, both $p < 0.01$).

We also recently developed a method to generate myeloid cells with a proliferative capacity from human iPS cells (44, 45). iPS cell–derived proliferating myeloid cell lines (iPS-ML) were generated by introducing proliferation and antisenescence factors (e.g., cMYC and BMI1) into human iPS cell–derived myeloid cells, and they grew continuously in an M-CSF–dependent manner. This technique enabled us to generate a large quantity of human cells exhibiting macrophage-like properties. We observed that iPS-ML genetically modified to express IFN-β significantly inhibited the growth of human gastric and pancreatic cancers in xenograft models using SCID mice (45). However, there are several drawbacks related to the application of iPS-ML in practical medicine. The generation of patient-specific iPS-ML may be very expensive, and >2 mo are necessary to establish iPS cells and subsequently generate iPS-ML. A more critical issue is the risk for developing malignancy after administration of autologous iPS-ML to patients.

TAP is a dimer composed of TAP1 and TAP2 molecules, and it plays a key role in the supply of antigenic peptides to the HLA class I pathway (46). In TAP-deficient cells, cell surface expression of HLA class I, as well as the diversity of peptides presented by HLA class I molecules, is very low. Thus, we expect that TAP-deficient allogeneic iPS-ML evade recognition by most allo-MHC class I–reactive CTL that play a major role in the acute rejection of transferred allogeneic cells (47, 48). Nevertheless, the alloreactive CTL recognizing HLA class I–bound peptides presented via the TAP-independent pathway, which are mainly derived from signal peptides of membrane or secreted proteins (49), may eventually eliminate the transferred allogeneic iPS-ML cells. Collectively, TAP-deficient allogeneic iPS-ML may survive in recipients for a certain duration and exert their anticancer effects, but eventually they would be eliminated by the immune system. Therefore, we presume that therapies using allogeneic TAP-deficient iPS-ML cells may be effective and safe.

In the current study, we evaluated this concept using a mouse model. We generated ES-ML from TAP1-deficient mouse E14 ES cells derived from the 129/sv strain with an H-2^b MHC haplotype. We demonstrated that treatment of cancer-bearing BALB/c mice (H-2^d) with TAP1-deficient ES-ML, with and without production of TNF, plus IFN-γ resulted in significant inhibition of cancer progression (Fig. 7), as well as prolongation of mouse survival (Fig. 8). These results indicate that TAP-deficient ES-ML can act as anticancer effector cells in H-2–mismatched recipients. Furthermore, as indicated by Supplemental Fig. 3, even if $>1.5 \times 10^8$ ES-ML were administered per mouse in total, we never observed development of malignancies from the transferred ES-ML.

The present study demonstrated that anticancer therapy using allogeneic TAP-deficient pluripotent stem cell–derived proliferating macrophages is effective and safe. We observed no malignancy development from TAP-mutated ES-ML after transfer to allogeneic recipient mice, as shown in Supplemental Fig. 3. We are planning a similar preclinical study using nonhuman primates to further evaluate the safety of macrophage therapy. Cancer therapy strategies using other cell types with tumor tropism, such as mesenchymal stem cells and neural stem cells, have been reported (50–53). These strategies will be evaluated further for their efficacy and safety in preclinical and clinical studies in the near future.

Disclosures

The authors have no financial conflicts of interest.

References

1. Lewis, C. E., and J. W. Pollard. 2006. Distinct role of macrophages in different tumor microenvironments. *Cancer Res.* 66: 605–612.
2. De Palma, M., and C. E. Lewis. 2013. Macrophage regulation of tumor responses to anticancer therapies. *Cancer Cell* 23: 277–286.
3. Coussens, L. M., L. Zitvogel, and A. K. Palucka. 2013. Neutralizing tumor-promoting chronic inflammation: a magic bullet? *Science* 339: 286–291.
4. Mantovani, A., T. Schioppa, C. Porta, P. Allavena, and A. Sica. 2006. Role of tumor-associated macrophages in tumor progression and invasion. *Cancer Metastasis Rev.* 25: 315–322.
5. Sica, A., and V. Bronte. 2007. Altered macrophage differentiation and immune dysfunction in tumor development. *J. Clin. Invest.* 117: 1155–1166.
6. Sica, A., and A. Mantovani. 2012. Macrophage plasticity and polarization: in vivo veritas. *J. Clin. Invest.* 122: 787–795.
7. Tsujikawa, T., T. Yaguchi, G. Ohmura, S. Ohta, A. Kobayashi, N. Kawamura, T. Fujita, H. Nakano, T. Shimada, T. Takahashi, et al. 2013. Autocrine and paracrine loops between cancer cells and macrophages promote lymph node metastasis via CCR4/CCL22 in head and neck squamous cell carcinoma. *Int. J. Cancer* 132: 2755–2766.
8. Bonnotte, B., N. Larmonier, N. Favre, A. Fromentin, M. Moutet, M. Martin, S. Gurbuxani, E. Solary, B. Chauffert, and F. Martin. 2001. Identification of tumor-infiltrating macrophages as the killers of tumor cells after immunization in a rat model system. *J. Immunol.* 167: 5077–5083.
9. Guiducci, C., A. P. Vicari, S. Sangaletti, G. Trinchieri, and M. P. Colombo. 2005. Redirecting in vivo elicited tumor infiltrating macrophages and dendritic cells towards tumor rejection. *Cancer Res.* 65: 3437–3446.
10. Hagemann, T., T. Lawrence, I. McNeish, K. A. Charles, H. Kulbe, R. G. Thompson, S. C. Robinson, and F. R. Balkwill. 2008. "Re-educating" tumor-associated macrophages by targeting NF-kappaB. *J. Exp. Med.* 205: 1261–1268.
11. Dace, D. S., P. W. Chen, and J. Y. Niederkorn. 2008. CD4+ T-cell-dependent tumour rejection in an immune-privileged environment requires macrophages. *Immunology* 123: 367–377.
12. Menon, C., T. W. Bauer, S. T. Kelley, D. J. Raz, J. I. Bleier, K. Patel, K. Steele, I. Prabakaran, A. Shifrin, D. G. Buerk, et al. 2008. Tumoricidal activity of high-dose tumor necrosis factor-alpha is mediated by macrophage-derived nitric oxide burst and permanent blood flow shutdown. *Int. J. Cancer* 123: 464–475.
13. Ho, T. C., S. L. Chen, S. C. Shih, S. J. Chang, S. L. Yang, J. W. Hsieh, H. C. Cheng, L. J. Chen, and Y. P. Tsao. 2011. Pigment epithelium-derived factor (PEDF) promotes tumor cell death by inducing macrophage membrane tumor necrosis factor-related apoptosis-inducing ligand (TRAIL). *J. Biol. Chem.* 286: 35943–35954.
14. Beatty, G. L., E. G. Chiorean, M. P. Fishman, B. Saboury, U. R. Teitelbaum, W. Sun, R. D. Huhn, W. Song, D. Li, L. L. Sharp, et al. 2011. CD40 agonists alter tumor stroma and show efficacy against pancreatic carcinoma in mice and humans. *Science* 331: 1612–1616.
15. Shirota, Y., H. Shirota, and D. M. Klinman. 2012. Intratumoral injection of CpG oligonucleotides induces the differentiation and reduces the immunosuppressive activity of myeloid-derived suppressor cells. *J. Immunol.* 188: 1592–1599.
16. Shime, H., M. Matsumoto, H. Oshiumi, S. Tanaka, A. Nakane, Y. Iwakura, H. Tahara, N. Inoue, and T. Seya. 2012. Toll-like receptor 3 signaling converts tumor-supporting myeloid cells to tumoricidal effectors. *Proc. Natl. Acad. Sci. USA* 109: 2066–2071.
17. Movahedi, K., D. Laoui, C. Gysemans, M. Baeten, G. Stangé, J. Van den Bossche, M. Mack, D. Pipeleers, P. In't Veld, P. De Baetselier, and J. A. Van Ginderachter. 2010. Different tumor microenvironments contain functionally distinct subsets of macrophages derived from Ly6C(high) monocytes. *Cancer Res.* 70: 5728–5739.
18. Murray, P. J., and T. A. Wynn. 2011. Protective and pathogenic functions of macrophage subsets. *Nat. Rev. Immunol.* 11: 723–737.
19. Faradji, A., A. Bohbot, M. Schmitt-Goguel, N. Roeslin, S. Dumont, M. L. Wiesel, C. Lallot, M. Eber, J. Bartholeyns, P. Poindron, et al. 1991. Phase I trial of intravenous infusion of ex-vivo-activated autologous blood-derived macrophages in patients with non-small-cell lung cancer: toxicity and immunomodulatory effects. *Cancer Immunol. Immunother.* 33: 319–326.
20. Lopez, M., J. Fechtenbaum, B. David, C. Martinache, M. Chokri, S. Canepa, A. De Gramont, C. Louvet, I. Gorin, O. Mortel, and J. Bartholeyns. 1992. Adoptive immunotherapy with activated macrophages grown in vitro from blood monocytes in cancer patients: a pilot study. *J. Immunother.* 11: 209–217.
21. Andreesen, R., C. Scheibenbogen, W. Brugger, S. Krause, H. G. Meerpohl, H. G. Leser, H. Engler, and G. W. Löhr. 1990. Adoptive transfer of tumor cytotoxic macrophages generated in vitro from circulating blood monocytes: a new approach to cancer immunotherapy. *Cancer Res.* 50: 7450–7456.
22. Baron-Bodo, V., P. Doceur, M. L. Lefebvre, K. Labroquère, C. Defaye, C. Cambouris, D. Prigent, M. Salcedo, A. Boyer, and A. Nardin. 2005. Antitumor properties of human-activated macrophages produced in large scale for clinical application. *Immunobiology* 210: 267–277.
23. Klimp, A. H., E. G. de Vries, G. L. Scherphof, and T. Daemen. 2002. A potential role of macrophage activation in the treatment of cancer. *Crit. Rev. Oncol. Hematol.* 44: 143–161.
24. Monnet, I., J. L. Breau, D. Moro, H. Lena, J. C. Eymard, O. Ménard, J. P. Vuillez, M. Chokri, J. L. Romet-Lemonne, and M. Lopez. 2002. Intrapleural infusion of activated macrophages and gamma-interferon in malignant pleural mesothelioma: a phase II study. *Chest* 121: 1921–1927.
25. Hennemann, B., A. Rehm, A. Kottke, N. Meidenbauer, and R. Andreesen. 1997. Adoptive immunotherapy with tumor-cytotoxic macrophages derived from recombinant human granulocyte-macrophage colony-stimulating factor (rhuGM-CSF) mobilized peripheral blood monocytes. *J. Immunother.* 20: 365–371.
26. Takahashi, K., K. Tanabe, M. Ohnuki, M. Narita, T. Ichisaka, K. Tomoda, and S. Yamanaka. 2007. Induction of pluripotent stem cells from adult human fibroblasts by defined factors. *Cell* 131: 861–872.
27. Senju, S., M. Haruta, Y. Matsunaga, S. Fukushima, T. Ikeda, K. Takahashi, K. Okita, S. Yamanaka, and Y. Nishimura. 2009. Characterization of dendritic cells and macrophages generated by directed differentiation from mouse induced pluripotent stem cells. *Stem Cells* 27: 1021–1031.
28. Senju, S., M. Haruta, K. Matsumura, Y. Matsunaga, S. Fukushima, T. Ikeda, K. Takamatsu, A. Irie, and Y. Nishimura. 2011. Generation of dendritic cells and macrophages from human induced pluripotent stem cells aiming at cell therapy. *Gene Ther.* 18: 874–883.
29. Choi, K. D., M. A. Vodyanik, and I. I. Slukvin. 2009. Generation of mature human myelomonocytic cells through expansion and differentiation of pluripotent stem cell-derived lin-CD34+CD43+CD45+ progenitors. *J. Clin. Invest.* 119: 2818–2829.
30. Yanagimachi, M. D., A. Niwa, T. Tanaka, F. Honda-Ozaki, S. Nishimoto, Y. Murata, T. Yasumi, J. Ito, S. Tomida, K. Oshima, et al. 2013. Robust and highly-efficient differentiation of functional monocytic cells from human pluripotent stem cells under serum- and feeder cell-free conditions. *PLoS ONE* 8: e59243.
31. Matsunaga, Y., D. Fukuma, S. Hirata, S. Fukushima, M. Haruta, T. Ikeda, I. Negishi, Y. Nishimura, and S. Senju. 2008. Activation of antigen-specific cytotoxic T lymphocytes by beta 2-microglobulin or TAP1 gene disruption and the introduction of recipient-matched MHC class I gene in allogeneic embryonic stem cell-derived dendritic cells. *J. Immunol.* 181: 6635–6643.
32. Senju, S., S. Hirata, H. Matsuyoshi, M. Masuda, Y. Uemura, K. Araki, K. Yamamura, and Y. Nishimura. 2003. Generation and genetic modification of dendritic cells derived from mouse embryonic stem cells. *Blood* 101: 3501–3508.
33. Song, E., P. Zhu, S. K. Lee, D. Chowdhury, S. Kussman, D. M. Dykxhoorn, Y. Feng, D. Palliser, D. B. Weiner, P. Shankar, et al. 2005. Antibody mediated in vivo delivery of small interfering RNAs via cell-surface receptors. *Nat. Biotechnol.* 23: 709–717.
34. Miyoshi, H., U. Blömer, M. Takahashi, F. H. Gage, and I. M. Verma. 1998. Development of a self-inactivating lentivirus vector. *J. Virol.* 72: 8150–8157.
35. Cohen, J. A., D. B. Weiner, K. F. More, Y. Kokai, W. V. Williams, H. C. Maguire, Jr., V. A. LiVolsi, and M. I. Greene. 1989. Expression pattern of the neu (NGL) gene-encoded growth factor receptor protein (p185neu) in normal and transformed epithelial tissues of the digestive tract. *Oncogene* 4: 81–88.
36. Kuwada, S. K., C. L. Scaife, J. Kuang, X. Li, R. F. Wong, S. R. Florell, R. J. Coffey, Jr., and P. D. Gray. 2004. Effects of trastuzumab on epidermal growth factor receptor-dependent and -independent human colon cancer cells. *Int. J. Cancer* 109: 291–301.
37. Carter, P., L. Presta, C. M. Gorman, J. B. Ridgway, D. Henner, W. L. Wong, A. M. Rowland, C. Kotts, M. E. Carver, and H. M. Shepard. 1992. Humanization of an anti-p185HER2 antibody for human cancer therapy. *Proc. Natl. Acad. Sci. USA* 89: 4285–4289.
38. Gravalos, C., and A. Jimeno. 2008. HER2 in gastric cancer: a new prognostic factor and a novel therapeutic target. *Ann. Oncol.* 19: 1523–1529.
39. Iannello, A., and A. Ahmad. 2005. Role of antibody-dependent cell-mediated cytotoxicity in the efficacy of therapeutic anti-cancer monoclonal antibodies. *Cancer Metastasis Rev.* 24: 487–499.
40. Stuehr, D. J., and M. A. Marletta. 1987. Induction of nitrite/nitrate synthesis in murine macrophages by BCG infection, lymphokines, or interferon-gamma. *J. Immunol.* 139: 518–525.
41. Ding, A. H., C. F. Nathan, and D. J. Stuehr. 1988. Release of reactive nitrogen intermediates and reactive oxygen intermediates from mouse peritoneal macrophages. Comparison of activating cytokines and evidence for independent production. *J. Immunol.* 141: 2407–2412.
42. Rees, D. D., R. M. Palmer, H. F. Hodson, and S. Moncada. 1989. A specific inhibitor of nitric oxide formation from L-arginine attenuates endothelium-dependent relaxation. *Br. J. Pharmacol.* 96: 418–424.

43. Pallasch, C. P., I. Leskov, C. J. Braun, D. Vorholt, A. Drake, Y. M. Soto-Feliciano, E. H. Bent, J. Schwamb, B. Iliopoulou, N. Kutsch, et al. 2014. Sensitizing protective tumor microenvironments to antibody-mediated therapy. *Cell* 156: 590–602.
44. Haruta, M., Y. Tomita, A. Yuno, K. Matsumura, T. Ikeda, K. Takamatsu, E. Haga, C. Koba, Y. Nishimura, and S. Senju. 2013. TAP-deficient human iPS cell-derived myeloid cell lines as unlimited cell source for dendritic cell-like antigen-presenting cells. *Gene Ther.* 20: 504–513.
45. Koba, C., M. Haruta, Y. Matsunaga, K. Matsumura, E. Haga, Y. Sasaki, T. Ikeda, K. Takamatsu, Y. Nishimura, and S. Senju. 2013. Therapeutic effect of human iPS-cell-derived myeloid cells expressing IFN-β against peritoneally disseminated cancer in xenograft models. *PLoS ONE* 8: e67567.
46. Neefjes, J. J., F. Momburg, and G. J. Hämmerling. 1993. Selective and ATP-dependent translocation of peptides by the MHC-encoded transporter. *Science* 261: 769–771.
47. Loyer, V., P. Fontaine, S. Pion, F. Hétu, D. C. Roy, and C. Perreault. 1999. The in vivo fate of APCs displaying minor H antigen and/or MHC differences is regulated by CTLs specific for immunodominant class I-associated epitopes. *J. Immunol.* 163: 6462–6467.
48. Hermans, I. F., D. S. Ritchie, J. Yang, J. M. Roberts, and F. Ronchese. 2000. CD8 + T cell-dependent elimination of dendritic cells in vivo limits the induction of antitumor immunity. *J. Immunol.* 164: 3095–3101.
49. Bacik, I., J. H. Cox, R. Anderson, J. W. Yewdell, and J. R. Bennink. 1994. TAP (transporter associated with antigen processing)-independent presentation of endogenously synthesized peptides is enhanced by endoplasmic reticulum insertion sequences located at the amino- but not carboxyl-terminus of the peptide. *J. Immunol.* 152: 381–387.
50. Studeny, M., F. C. Marini, R. E. Champlin, C. Zompetta, I. J. Fidler, and M. Andreeff. 2002. Bone marrow-derived mesenchymal stem cells as vehicles for interferon-beta delivery into tumors. *Cancer Res.* 62: 3603–3608.
51. Hall, B., J. Dembinski, A. K. Sasser, M. Studeny, M. Andreeff, and F. Marini. 2007. Mesenchymal stem cells in cancer: tumor-associated fibroblasts and cell-based delivery vehicles. *Int. J. Hematol.* 86: 8–16.
52. Aboody, K. S., J. Najbauer, and M. K. Danks. 2008. Stem and progenitor cell-mediated tumor selective gene therapy. *Gene Ther.* 15: 739–752.
53. Ren, C., S. Kumar, D. Chanda, J. Chen, J. D. Mountz, and S. Ponnazhagan. 2008. Therapeutic potential of mesenchymal stem cells producing interferon-alpha in a mouse melanoma lung metastasis model. *Stem Cells* 26: 2332–2338.

OncoImmunology 3, e27927; January 2014; © 2014 Landes Bioscience

Application of iPS cell-derived macrophages to cancer therapy

Satoru Senju[1,2,*], Chihiro Koba[1,2], Miwa Haruta[1,2], Yusuke Matsunaga[1,2], Keiko Matsumura[1,2], Eriko Haga[1,2], Yuko Sasaki[1,2], Tokunori Ikeda[1,2], Koutaro Takamatsu[1,2], and Yasuharu Nishimura[1]

[1]Department of Immunogenetics; Graduate School of Medical Sciences; Kumamoto University; Kumamoto, Japan;
[2]CREST; Japan Science and Technology Agency; Kawaguchi, Japan

Keywords: gastric cancer, interferon β, iPS cells, macrophages, pancreatic cancer, peritoneal dissemination

We established a method to produce a large quantity of myeloid cells from human inducible pluripotent stem cells (iPSCs). When injected intraperitoneally into mice carrying established peritoneal tumors, iPSC-derived myeloid cells (iPS-MCs) efficiently accumulated within neoplastic lesions. The intraperitoneal injection of iPS-MCs expressing interferon β significantly inhibited the growth of human gastric and pancreatic cancers implanted in the peritoneal cavity of immunocompromised mice.

Introduction

Macrophage infiltration is frequently observed in solid tumors.[1] Recent studies indicate that tumor-associated macrophages (TAMs) are significantly involved in tumor progression, accelerating the local invasion and metastatic dissemination of malignant cells.[2] Other studies have highlighted the possibility that macrophages may also mediate a tumoricidal effect, leading to the development of macrophage-based anticancer therapies. As a standalone example, the transfer of autologous monocyte-derived macrophages activated with interferon (IFN) γ ex vivo has been tested as a potential intervention for patients with solid tumors.[3] However, no clear therapeutic benefit has thus far associated with macrophage-based anticancer therapies. To optimize the efficacy of such an approach, improvements of the method for supplying macrophages are necessary. Indeed, if sufficient amounts of macrophages exerting potent anticancer effects could be repeatedly administered, patients may achieve robust clinical benefit from this cell-based immunotherapeutic regimen.

iPSC-Derived Proliferating Myeloid Cells

Several groups, including ours, have thus far established methods to generate macrophages from mouse or human inducible pluripotent stem cells (iPSCs).[4,5] However, the number of macrophages generated from human iPSCs is only 10–20 times higher than the number of undifferentiated iPSCs used as starting material. In addition, the generation of macrophages from iPSCs is time-consuming, laborious, and too expensive to be applied to the clinical practice.

Recently, we established a method to induce proliferation of the iPSC–derived myeloid cells (iPS-MCs) by the lentivirus-mediated transduction of genes that promote cell proliferation or inhibit cell senescence, *i.e.*, *v-myc* avian myelocytomatosis viral oncogene homolog (*MYC*) plus *BMI1*, to generate an iPSC-derived myeloid/macrophage cell line (iPS-ML). Such an iPS-ML can proliferate in a colony stimulating factor 1 (CSF1)-dependent manner for at least several months while retaining the potential to differentiate into dendritic cells (iPS-ML-DCs) with a potent T cell-stimulating capacity.[6]

Accumulation and Infiltration of Intraperitoneally Injected iPS-ML in Tumor Tissues

We examined whether or not iPS-ML administered intraperitoneally would infiltrate tumor lesions pre-established in the peritoneal cavity of mice.[7] To this end, green fluorescent protein (GFP)-expressing NUGC-4 human gastric cancer cells, which have been established from a peritoneal metastatic lesion removed from an individual with diffuse gastric cancer, were intraperitoneally injected into SCID mice. After 15 d, iPS-ML labeled with the red fluorescent dye PKH26 were administered via the same route. Macroscopic fluorescence analysis on the next day revealed that both NUGC-4-derived tumors and iPS-ML localize for the most part to the greater omentum, demonstrating that iPS-ML efficiently accumulate into neoplastic lesions. Of note, such a preferential accumulation of iPS-ML into the greater omentum was not observed when

*Correspondence to: Satoru Senju; Email: senjusat@gpo.kumamoto-u.ac.jp
Submitted: 01/21/2014; Accepted: 01/21/2014; Published Online: 02/14/2014
Citation: Senju S, Koba C, Haruta M, Matsunaga Y, Matsumura K, Haga E, Sasaki Y, Ikeda T, Takamatsu K, Nishimura Y. Application of iPS cell-derived macrophages to cancer therapy. OncoImmunology 2014; 3:e27927; http://dx.doi.org/10.4161/onci.27927

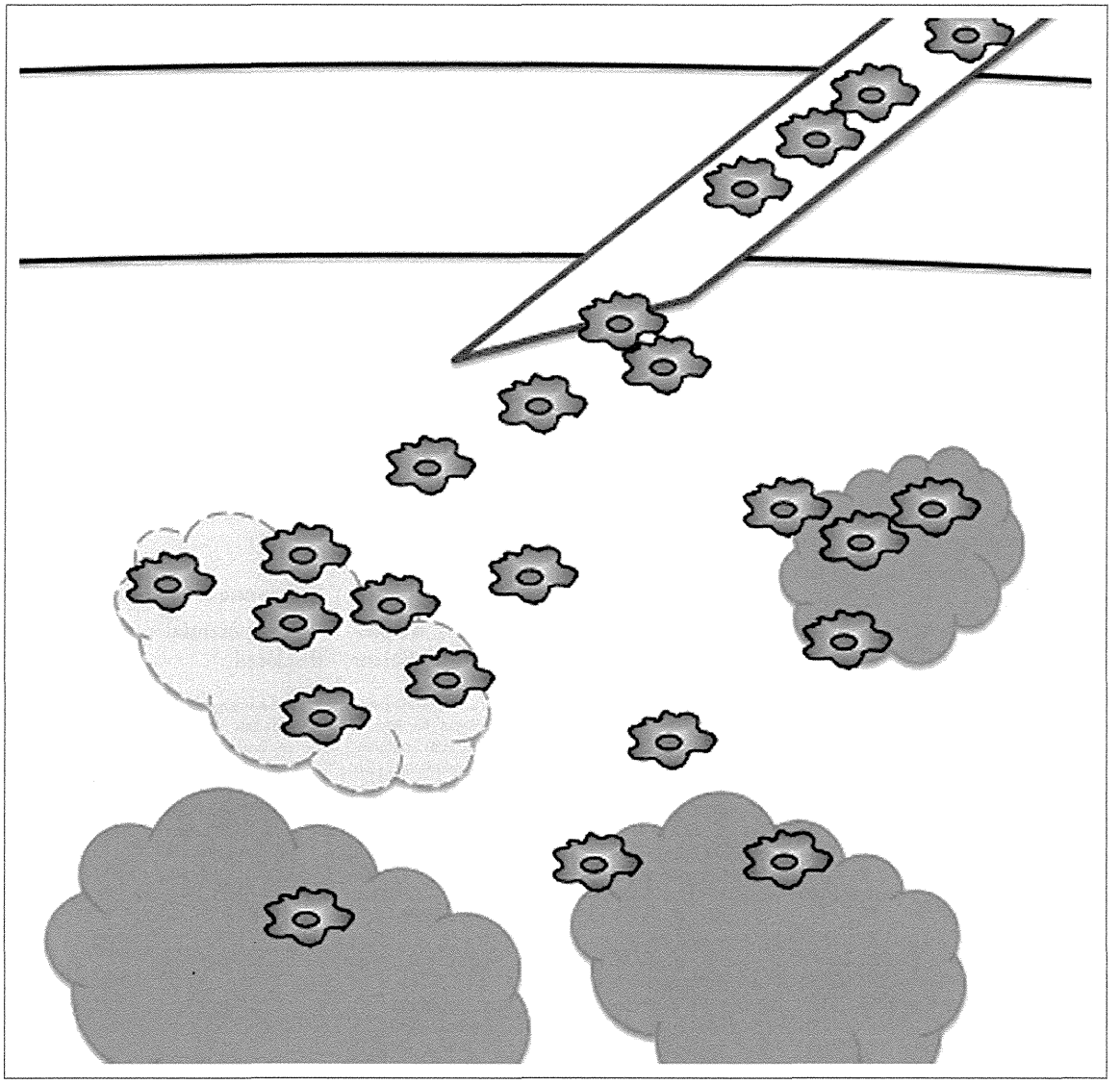

Figure 1. Anticancer therapy with iPSC-derived macrophages producing interferon β. Inducible pluripotent stem cell (iPSC)-derived myeloid cells (iPS-MCs) infiltrate tumor tissues upon injection into cancer-bearing recipients. Interferon β (IFNβ)-expressing iPS-MCs secrete IFNβ within neoplastic lesions, hence causing disease regression.

iPS-ML were inoculated into tumor-free mice. Next, we isolated and microscopically examined neoplastic lesions. PKH26-labeled iPS-ML infiltrated nests of GFP-expressing NUGC-4 cells. Higher magnification analysis of tumor sections clearly demonstrated the infiltration of iPS-ML into the neoplastic tissue. These results indicate that iPS-ML efficiently infiltrate malignant tissues when intraperitoneally injected into mice carrying cancers established in the peritoneal cavity.

Therapeutic Effects of IFNβ-Secreting iPS-ML on Peritoneally Disseminated NUGC-4 Gastric Cancer Cells in Xenograft Models

IFNβ exerts anti-proliferative and/or pro-apoptotic effects on various types of cancer cells. We examined the effects of iPS-ML genetically modified to secrete IFNβ (iPS-ML/IFNβ) against NUGC-4 cells in vivo.[7] We generated NUGC-4 cells expressing the firefly luciferase, NUGC4/Luc cells, which can be easily monitored in vivo by bioluminescence analysis. SCID mice were then inoculated with NUGC-4/Luc cells (day 0), and 4 d later they were divided into a treated and a control group. Mice belonging to the treated group were injected *i.p.* with iPS-ML/IFNβ from day 4 (2×10^7 cells/injection/mouse, 3 injections per week). Tumor growth was significantly inhibited by the inoculation of iPS-ML/IFNβ cells. Of note, the administration of iPS-ML/IFNβ also inhibited the growth of MIAPaCa-2 pancreatic cancer cells in a similar xenograft model.

In summary, iPS-MCs expressing IFNβ potently inhibit the growth of human gastric and pancreatic cancers growing in immunocompromised SCID mice.

Toward Clinical Applications

Gastric cancer is one of most frequent malignancies worldwide and the second most frequent cause of cancer-related mortality. Peritoneal dissemination is the most difficult type of metastasis to treat of those associated with gastric cancer. Pancreatic cancer has a poor prognosis, with overall 5-y survival rate being < 10%. Thus, efficient therapies for these intractable cancers are urgently needed. The present study suggests that iPS-MCs secreting antineoplastic factors may be used to treat cancers for which no standard therapy has been established yet.

For macrophage-based immunotherapeutic regimens to achieve robust clinical effects, cancer patients may need to receive repetitive administrations of large numbers of cells. Since our iPS-ML proliferates for at least several months, sufficient amounts of iPS-MCs may be readily available by this approach. However, the proliferative capacity of our iPS-ML may constitute a concern, as this line could drive leukemogenesis, at least theoretically, in a completely autologous setting.

To circumvent such risk, we plan to use allogeneic iPS-ML lacking transporter associated with antigen presentation (TAP) for future clinical applications. TAP plays a key role in antigen-presentation by MHC class I molecules. In TAP-deficient cells, the expression levels of MHC class I molecules on the cell surface are very low. More importantly, the lack of TAP greatly reduces the complexity of peptides presented on MHC class I molecules. In line with these notions, we previously demonstrated that TAP-deficient cells evade recognition by most alloreactive $CD8^+$ T cells (the major immune effector cells mediating acute rejection) upon transfer into allogeneic recipients.[8] Nevertheless, alloreactive $CD8^+$ T cells recognizing MHC class I-bound peptides presented via the TAP-independent pathway (mainly derived from signal peptides) may eventually eliminate the allogeneic TAP-deficient iPS-MCs. Based on these premises, we predict that TAP-deficient iPS-MCs would survive in the recipient for several days, allowing them to exert anticancer effects, but would then be eliminated by the recipient's immune system. Thus, the administration of allogeneic, TAP-deficient iPS-MCs to cancer patients should be effective and safe. (**Fig. 1**)

Disclosure of Potential Conflicts of Interest

No potential conflicts of interest were disclosed.

References

1. Lewis CE, Pollard JW. Distinct role of macrophages in different tumor microenvironments. Cancer Res 2006; 66:605-12; PMID:16423985; http://dx.doi.org/10.1158/0008-5472.CAN-05-4005
2. Mantovani A, Schioppa T, Porta C, Allavena P, Sica A. Role of tumor-associated macrophages in tumor progression and invasion. Cancer Metastasis Rev 2006; 25:315-22; PMID:16967326; http://dx.doi.org/10.1007/s10555-006-9001-7
3. Andreesen R, Hennemann B, Krause SW. Adoptive immunotherapy of cancer using monocyte-derived macrophages: rationale, current status, and perspectives. J Leukoc Biol 1998; 64:419-26; PMID:9766621
4. Choi KD, Vodyanik MA, Slukvin II. Generation of mature human myelomonocytic cells through expansion and differentiation of pluripotent stem cell-derived lin-CD34+CD43+CD45+ progenitors. J Clin Invest 2009; 119:2818-29; PMID:19726877; http://dx.doi.org/10.1172/JCI38591
5. Senju S, Haruta M, Matsumura K, Matsunaga Y, Fukushima S, Ikeda T, Takamatsu K, Irie A, Nishimura Y. Generation of dendritic cells and macrophages from human induced pluripotent stem cells aiming at cell therapy. Gene Ther 2011; 18:874-83; PMID:21430784; http://dx.doi.org/10.1038/gt.2011.22
6. Haruta M, Tomita Y, Yuno A, Matsumura K, Ikeda T, Takamatsu K, Haga E, Koba C, Nishimura Y, Senju S. TAP-deficient human iPS cell-derived myeloid cell lines as unlimited cell source for dendritic cell-like antigen-presenting cells. Gene Ther 2013; 20:504-13; PMID:22875043; http://dx.doi.org/10.1038/gt.2012.59
7. Koba C, Haruta M, Matsunaga Y, Matsumura K, Haga E, Sasaki Y, Ikeda T, Takamatsu K, Nishimura Y, Senju S. Therapeutic effect of human iPS-cell-derived myeloid cells expressing IFN-β against peritoneally disseminated cancer in xenograft models. PLoS One 2013; 8:e67567; PMID:23826321; http://dx.doi.org/10.1371/journal.pone.0067567
8. Matsunaga Y, Fukuma D, Hirata S, Fukushima S, Haruta M, Ikeda T, Negishi I, Nishimura Y, Senju S. Activation of antigen-specific cytotoxic T lymphocytes by beta 2-microglobulin or TAP1 gene disruption and the introduction of recipient-matched MHC class I gene in allogeneic embryonic stem cell-derived dendritic cells. J Immunol 2008; 181:6635-43; PMID:18941254

Clinical Cancer Research

Phase II Clinical Trial of Multiple Peptide Vaccination for Advanced Head and Neck Cancer Patients Revealed Induction of Immune Responses and Improved OS

Yoshihiro Yoshitake[1,2], Daiki Fukuma[1], Akira Yuno[1,3], Masatoshi Hirayama[1,3], Hideki Nakayama[1], Takuya Tanaka[1], Masashi Nagata[1,4], Yasuo Takamune[1], Kenta Kawahara[1], Yoshihiro Nakagawa[1], Ryoji Yoshida[1], Akiyuki Hirosue[1], Hidenao Ogi[1], Akimitsu Hiraki[1], Hirofumi Jono[5], Akinobu Hamada[5,6], Koji Yoshida[7,8], Yasuharu Nishimura[3], Yusuke Nakamura[9], and Masanori Shinohara[1]

Abstract

Purpose: The peptides derived from ideal cancer–testis antigens, including LY6K, CDCA1, and IMP3 (identified using genome-wide cDNA microarray analyses), were used in immunotherapy for head and neck squamous cell cancer (HNSCC). In this trial, we analyzed the immune response to and safety and efficacy of vaccine therapy.

Experimental Design: A total of 37 patients with advanced HNSCC were enrolled in this trial of peptide vaccine therapy, and the OS, PFS, and immunologic response were evaluated using enzyme-linked ImmunoSpot (ELISPOT) and pentamer assays. The peptides were subcutaneously administered weekly with IFA. The primary endpoints were evaluated on the basis of differences between *HLA-A*2402*-positive [A24(+)] patients treated with peptide vaccine therapy and -negative [A24(−)] patients treated without peptide vaccine therapy among those with advanced HNSCC.

Results: Our cancer vaccine therapy was well tolerated. The OS of the A24(+) vaccinated group ($n = 37$) was statistically significantly longer than that of the A24(−) group ($n = 18$) and median survival time (MST) was 4.9 versus 3.5 months, respectively; $P < 0.05$. One of the patients exhibited a complete response. In the A24(+) vaccinated group, the ELISPOT assay identified LY6K-, CDCA1-, and IMP3-specific CTL responses in 85.7%, 64.3%, and 42.9% of the patients, respectively. The patients showing LY6K- and CDCA1-specific CTL responses demonstrated a longer OS than those without CTL induction. Moreover, the patients exhibiting CTL induction for multiple peptides demonstrated better clinical responses.

Conclusions: The immune response induced by this vaccine may improve the prognosis of patients with advanced HNSCC. *Clin Cancer Res; 21(2); 312–21. ©2014 AACR.*

Introduction

Head and neck cancer (HNC) is the sixth most common type of cancer, representing approximately 6% of all cases and accounting for an estimated 650,000 new cancer cases and 350,000 cancer-related deaths worldwide every year (1–3); however, the disease carries a very poor prognosis. The 5-year survival among all stages of disease is approximately 60% (4). In the past decade, the treatment of locoregional advanced HNC has shifted from primary surgery to organ preservation using combination chemoradiotherapy (CRT). The current approach attempts to achieve both organ preservation and function with outcomes superior to radiotherapy alone or surgery with postoperative radiotherapy (5–11). Despite the use of aggressive treatment modalities, such as surgical tumor resection with radical neck dissection and chemoradiotherapy, maintaining long-term disease control of advanced HNC remains difficult. Some chemoradiotherapy regimens have a higher treatment effect; however, the 5-year survival rates have not been extended (12). One reason for the poor prognosis of HNC is the limited availability of treatment options for advanced disease. Although various drugs are used in chemotherapy and intensity modulated radiation therapy (IMRT), no

[1]Department of Oral and Maxillofacial Surgery, Graduate School of Medical Sciences, Kumamoto University, Kumamoto, Japan. [2]Itoh Dento-Maxillofacial Hospital, Kumamoto, Japan. [3]Department of Immunogenetics, Graduate School of Medical Sciences, Kumamoto University, Kumamoto, Japan. [4]Minamata City General Hospital and Medical Center, Minamata, Japan. [5]Department of Pharmacy, Kumamoto University Hospital and Department of Clinical Pharmaceutical Sciences, Graduate School of Pharmaceutical Sciences, Kumamoto University, Kumamoto, Japan. [6]Department of Clinical Pharmacology Group for Translational Research Support Core National Cancer Center Research Institute, Tokyo, Japan. [7]Laboratory of Molecular Medicine, Human Genome Center, Institute of Medical Science, University of Tokyo, Tokyo, Japan. [8]OncoTherapy Science Incorporation, Research and Development Division, Kanagawa, Japan. [9]Department of Medicine, University of Chicago, Chicago, Illinois.

Note: Supplementary data for this article are available at Clinical Cancer Research Online (http://clincancerres.aacrjournals.org/).

Corresponding Author: Yoshihiro Yoshitake, Department of Oral and Maxillofacial Surgery, Graduate School of Medical Sciences, Kumamoto University, Honjo 1-1-1 Chuo-ku, Kumamoto 860-8556, Japan. Phone: 81-96-373-5288; Fax: 81-96-373-5286; E-mail: yyoshi326@gmail.com

doi: 10.1158/1078-0432.CCR-14-0202

Translational Relevance

Cancer vaccination that induces cytotoxic T lymphocytes (CTL) to cancer–testis antigens is a potentially attractive option for the treatment of head and neck cancer (HNC). However, to date, immunotherapy using cancer–testis (CT) antigen–derived peptides has not demonstrated a correlation between the immune response and antitumor efficacy in clinical trials of advanced HNC. The peptides derived from three CT antigens used in this clinical trial are ideal targets for anticancer immunotherapy against HNC because they are specifically overexpressed in cancer cells, but not many normal tissues. In this phase II clinical trial of 37 patients with head and neck squamous cell cancer (HNSCC), we investigated the safety of and clinical and immunologic responses to these peptide vaccines. Our results showed peptide-specific CTLs in the peripheral blood of the patients with advanced HNSCC and increased $CD8^+$ T cell infiltration in the tumors following peptide vaccination. In addition, significantly, a CR was obtained after peptide vaccination in 1 patient who showed no effects after chemoradiotherapy or surgery. Furthermore, this is the first study to demonstrate that the peptide-specific CTL frequency is correlated with the overall survival in patients with HNSCC receiving peptide vaccination. These findings promote the use of peptide vaccination for the treatment of HNSCC.

molecular targeting agents against HNC have been developed, except for cetuximab. Therefore, the development of novel treatment modalities, such as immunotherapy, is eagerly awaited.

Immunotherapy is a potentially attractive treatment option for HNC. Some tumor-associated antigens (TAA) identified in HNC cells have the potential to be used in peptide-based vaccines. However, immunotherapy using TAA-derived peptides has not demonstrated adequate antitumor efficacy in clinical trials of advanced HNC. In this clinical trial, we used peptides derived from LY6K, CDCA1, and IMP3. All antigens used in this study were cancer–testis antigens, which are ideal targets for anticancer immunotherapy because they are particularly overexpressed in cancer cells and testis, a site of immune privilege, but not in other normal tissues, and promote the proliferation of cancer cells (13–16). We identified LY6K 177-186 (RYCNLEGPPI), CDCA1 56-64 (VYGIRLEHF), and IMP3 508-516 (KTVNELQNL) peptides that can induce peptide-reactive and HLA-A24 (*A*24:02*)-restricted cytotoxic T lymphocytes (CTL) without stimulating autoimmunity. HLA-A24 is the most common *HLA class I* allele in the Japanese population, and 60% of Japanese individuals (95% of whom have an *A*24:02* genotype), 20% of Caucasians, and 12% of Africans are positive for *HLA-A24* (17, 18). A phase II clinical cancer vaccination trial using a combination of multiple peptides derived from LY6K, TTK, and IMP3 in *HLA-A*24:02*(+) patients with advanced esophageal squamous cell carcinoma (ESCC) refractory to standard ESCC therapy was recently performed (14, 19), and the evidence from which encouraged us to develop this therapy against HNSCC for an evaluation in a phase II trial.

In this study, we evaluated the immunologic responses to and safety and survival benefits of cancer vaccination in a phase II trial of patients with advanced HNSCC refractory to standard therapy.

Materials and Methods

Study design

The present study is a phase II, open-label, nonrandomized clinical cancer vaccination trial conducted in an exploratory setting. The endpoints were evaluated on the basis of differences between the *HLA-A*24:02*-positive [A24(+)] and -negative [A24 (−)] groups as a biologic marker for the subgroup analysis. Vaccination with a mixture of multiple peptides derived from LY6K, CDCA1, and IMP3 and incomplete Freund's adjuvant (IFA; Montanide ISA51, SEPPIC) was performed in patients with HNSCC ($n = 37$) with locally advanced, recurrent, and/or metastatic tumors resistant to standard therapy. *HLA-A* genotyping was performed in all enrolled patients at the HLA Laboratory (Kyoto, Japan) according to the middle resolution genotyping method.

The primary endpoint in this study was overall survival (OS). The secondary endpoints were progression-free survival (PFS), immunologic responses, and adverse effects. Toxicities caused by the vaccination therapy were assessed according to the Common Terminology Criteria for Adverse Events version 3 (CTCAE). Immunologic monitoring was performed at the central laboratory using both enzyme-linked immunospot (ELISPOT) assays and HLA-A24/TAA peptide pentamer assays with the *in vitro* culture of lymphocytes derived from PBMCs at the pre- and postvaccination periods, as described below. The OS, which was measured as the period until death from the day on which the patient received a terminal prognosis, was analyzed according to the Kaplan–Meier method, and the PFS was calculated to assess disease progression.

The assessment of the endpoints was performed using an intention-to-treat analysis. This trial was approved by the institutional review board of Kumamoto University (Approval number at Kumamoto University of Principal Investigator, No. 841) and registered with the University Hospital Medical Information Network Clinical Trials Registry (UMIN-CTR) number, 000008379 (CTR-8379). Written informed consent was obtained from all participants. The trial was carried out in accordance with the Helsinki declaration regarding experimentation on human subjects.

Patient eligibility

The eligibility criteria for the patients participating in the clinical trial were as follows: (i) patients with HNSCC with locally advanced, recurrent and/or metastatic tumors who had failed to respond to standard therapy; (ii) adequate bone marrow, cardiac, pulmonary, hepatic and renal functions, including a WBC of $\geq$2,000/μL, a platelet count of $\geq$75,000/μL, a total bilirubin level of $\leq$2.0 of the institutional upper limit of normal, AST, ALT, and ALP levels of less than 2.5 times the institutional upper limits of normal and a creatinine level of $\leq$1.5 of the institutional upper limit of normal; (iii) no history of therapy within the 4 weeks before the initiation of the trial; (iv) an ECOG performance status (PS) of 0–2; and (v) an age of 18 to 85 years. The exclusion criteria were as follows: (i) pregnancy (including the refusal or inability to use effective means of contraception among females of childbearing potential); (ii) currently breastfeeding; (iii) serious bleeding disorders; (iv) serious infections requiring antibiotics; (v) concomitant treatment with steroids or immunosuppressive agents; and (vi) a determination of unsuitableness by the principal investigator or physician-in-charge.

In this study, none of the patients were excluded from these criteria.

Treatment protocol

Each of the three peptides (1 mg each) was emulsified in 1 mL of IFA and injected into the bilateral armpits. The vaccination was given subcutaneously once a week for 8 weeks. After that, they were vaccinated at every 4 weeks based on the detection of PD or the doctor's assessment. For the immunologic evaluation, PBMCs were obtained from the patients at the prevaccination period and after the fourth and eighth vaccinations. For the imaging analysis, CT was performed during the prevaccination period (within 1 month before vaccination) and at every four vaccinations.

Peptides

Peptides derived from LY6K-177 (RYCNLEGPPI), CDCA1-64 (VYGIRLEHF), and IMP3-508 (KTVNELQNL) able to induce tumor-reactive and HLA-A24 (*A*24:02*)-restricted CTLs were synthesized as described elsewhere (14). The purity (>97%) of the peptides was determined using analytic high-performance liquid chromatography (HPLC) and mass spectrometry. The endotoxin levels and bioburden of the peptides were tested and determined to be within acceptable ranges of the GMP grade for vaccination (NeoMPS, Inc.).

Lymphocyte preparation for immunologic monitoring

The protocol for the immunologic assay performed at the central laboratory was periodically standardized and validated according to the Clinical Laboratory Improvements Amendments (CLIA) and International Conference on Harmonization of Technical Requirements for the Registration of Pharmaceuticals for Human Use (ICH) guidelines (20, 21).

PBMCs were obtained from the patients during the prevaccination period and after the fourth and eighth vaccinations. Peripheral blood was obtained via venipuncture, collected in EDTA tubes, and transferred to the central laboratory at room temperature. Within 24 hours of blood collection, PBMCs were isolated using the Ficoll–Paque Plus (GE Healthcare Bio-sciences) density-gradient solution and stored at −80°C in cell stock media (Juji field) without serum at 5×10^6 cells/mL. After thawing, the degree of cell viability was confirmed to be more than 90% according to a trypan blue dye exclusion assay.

For the *in vitro* culture, the PBMCs were thawed simultaneously, and 5×10^5 cells per well were incubated in medium containing 100 units/mL of recombinant IL2 (rIL2; Novartis) with peptide stimulation (10 μg/mL) performed twice on days 1 and 8 in combination with HIV-specific peptide (ILKEPVHGV, 10 μg/mL) as a negative control and CMV-specific peptide (RYLRDQQLL, 10 μg/mL) as a positive control. On day 15, the cultured lymphocytes were subjected to an ELISPOT assay and a flow cytometry analysis after a depletion of $CD4^+$ cells using magnetic beads (Invitrogen). A conventional ELISPOT assay using TISI cells, a human B-lymphoblastoid cell line expressing HLA-A24, pulsed with the relevant peptide as a target in combination with an irrelevant HIV-specific peptide as a negative control was performed, followed by the HLA-A24/TAA peptide pentamer assay, as described below.

ELISPOT assay

To monitor the antigen-specific immune response, an ELISPOT assay was performed using the human IFN-γ ELISPOT PLUS kit (Mabtech). Ninety-six–well plates with nitrocellulose membranes (Millipore) were precoated with primary anti–IFN-γ antibodies (1-D1K) at 4°C overnight. The plates were then prereacted with RPMI-1640 medium containing 10% FBS (Invitrogen). Each vaccine peptide (10 μg/mL)-, HIV-specific peptide (ILKEPVHGV, 10 μg/mL)-, or CMV-specific peptide (RYLRDQQLL, 10 μg/mL)-pulsed TISI cells (2×10^4 per well) as stimulators, was incubated for 24 hours in triplicate with responder cells (from 2×10^4 per well to 2.5×10^3 per well) for a total of 200 μL/well in different responder/stimulator ratios, as indicated. Stimulation with phorbol 12-myristate 13-acetate (PMA; 25 ng/mL; Sigma-Aldrich) + ionomycin (500 pmol/L; Sigma-Aldrich) was used as a positive control for T-cell activation. The cell mixtures were treated with biotinylated secondary anti–IFN-γ antibodies (7-B6-1) and incubated for 2 hours. The plates were then incubated with HRP reagent and stained with TMB (Mabtech). The spots were quantified using an auto-analyzing system, the ImmunoSPOT S4 (Cellular Technology Ltd). Positivity for an antigen-specific T-cell response was quantitatively defined according to our original evaluation tree algorithm (19). In brief, the number of peptide-specific spots was calculated as the average of triplicates by subtracting the number of spots in the HIV peptide–pulsed stimulator well from that observed in the immunized peptide-pulsed stimulator well. Positivity for an antigen-specific T-cell response was classified into four grades (−, +, ++, and +++) depending on the number and variability of peptide-specific spots at different responder/stimulator ratios. When the algorithm indicated +, ++, or +++ at either the fourth or eighth vaccination point, we judged the case to be positive.

Pentamer staining and flow cytometry analysis

The *in vitro* cultured T cells were subjected to a pentamer assay to confirm peptide specificity. HLA-A24/LY6K-, /CDCA1- or /IMP3-peptides pentamer (ProImmune) staining in combination with anti-CD8 and anti-CD3 mAb staining was performed, and the results were analyzed using flow cytometry. Analysis of the frequency of Treg cells in the peripheral blood cells was performed using a FACSCalibur (Becton Dickinson). Frozen PBMC samples derived from patients before vaccination and at 7 days after the fourth and eighth vaccinations were thawed and directly used for detection of Treg cells. In this experiment, $CD4^+$ $CD25^{high}Foxp3^+$ cells were judged as Treg cells. The antibodies used to detect Treg cells were as follows: CD4-fluorescein isothiocyanate, Foxp3-phycoerythrin, and CD25-Allophycocyanin (eBioscience).

Immunohistochemical analysis of p16INK4A expression in cancer tissues

Immunohistochemical analysis of HPV p16INK4A expression was performed on formalin-fixed paraffin-embedded oral cancer tissue sections derived from 28 independent patients investigated in this clinical trial using the CINtec p16INK4A assay (Ventana Medical Systems, Inc.), according to the manufacturer's instructions. Cervical cancer tissue sections known to be HPV-positive were used as a positive control, and an omission of primary anti-HPV antibody was used as a negative control.

Statistical analysis

The OS and PFS were analyzed according to the Kaplan–Meier method, and statistical differences were assessed using the log-rank test. All statistical analyses were performed using the SPSS statistics 21.0 software package (SPSS, Inc.).

Results

Patient characteristics

We recruited 55 eligible patients with HNSCC between December 1, 2008 and December 5, 2012. A total of 37 patients were enrolled in this study (Supplementary Table S1). The background characteristics of the patients were not statistically different between the *HLA-A*24:02*-positive group ($n = 37$) treated with peptide vaccination and the *HLA-A*24:02*-negative group ($n = 18$) that received best supportive care. The median follow-up period was 4.3 months (range, 0.3–54.2 months). Of the 55 patients, 39 were male. The average age was 65 years (range, 36–85 years). A total of 3 patients had a PS of 2, 44 patients had a PS of 1, and 8 patients had a PS of 0. Staging was performed according to the TNM classification for HNC; 54 patients were diagnosed with stage IV disease and 1 patient was diagnosed with stage III disease. A total of 38 patients had undergone conventional chemotherapy, radiotherapy, and surgery, 13 patients had undergone chemotherapy and radiotherapy, 1 patient had undergone chemotherapy only, 1 patient had undergone radiotherapy only, and 2 patients had not received any treatment before the peptide vaccine therapy.

We investigated the expression of HPV-associated protein in oral squamous cell cancer tissues derived from 28 patients investigated in this study. We performed immunohistochemical staining of p16INK4A, which is the most reliable surrogate marker for HPV infection, as reported by Vermorken and colleagues (22, 23). Among the 28 cancer patients investigated, the 4 cases were maxillary gingival cancer, 11 cases were mandibular gingival cancer, 9 cases were tongue cancer, 3 cases were buccal mucosal cancer, and 1 case was oropharyngeal cancer. A positive staining of p16INK4A was observed in only 1 patient (case 24) of tongue cancer. The other 27 cases were negative for p16INK4A expression. Therefore, we suggest that there is no correlation between HPV infection status of oral cancer cells and the effects of peptides vaccination at least in our present study.

Clinical response, OS, and PFS

The characteristics and clinical responses of the patients treated with peptide vaccination ($n = 37$) are shown in Table 1. Among

Table 1. HNSCC patient characteristics, clinical response, and immune response of CTL

Patient no.	Age/sex	PS	Primary lesion	Stage[a]	Prior therapy[b]	Clinical response[c]	PFS (mo)	OS (mo)	CTL response[d]	Between (x) and (y)[e]
1	82/M	1	Mandibular gingiva	IV	Ope, CDDP, RT	SD	2.3	7.4	1 Ag	4W
2	68/M	1	Mandibular gingiva	IV	S-1	SD	5.2	11.6	2 Ag	4W
3	61/M	1	Pharynx	IV	Ope, S-1, CDDP, DTX, RT	SD	4.9	4.9	1 Ag	4W
4	61/M	1	Pharynx	IV	CDDP, 5FU, RT	PD	1.2	5.1	2 Ag	4W
5	71/M	1	Mandibular gingiva	IV	Ope, S-1,CDDP, RT	SD	2.4	2.4	NA	4W
6	40/M	1	Tongue	IV	S-1, CDDP, DTX, 5FU, RT	PD	1.2	1.2	NA	4W
7	54/F	1	Pharynx	IV	Ope, CDDP, RT	SD	12.4	12.4	2 Ag	4W
8	74/M	1	Mandibular gingiva	IV	Ope, DTX, RT	PD	2.1	2.1	NA	4W
9	58/M	0	Tongue	III	CDDP, RT	SD	12.6	54.2	3 Ag	4W
10	56/M	1	Pharynx	IV	Ope, S-1, CDDP, DTX, 5FU, RT	PD	1.4	1.4	NA	4W
11	68/M	1	Pharynx	IV	Ope, S-1, CDDP, DTX, RT	PD	1.7	1.7	1 Ag	4W
12	57/M	1	Tongue	IV	Ope, S-1, CDDP, DTX, 5FU, RT	PD	1.9	3	1 Ag	4W
13	68/M	0	Buccal mucosa	IV	Ope, S-1, DTX, RT	PD	1.9	6.8	2 Ag	4W
14	68/F	1	Maxillary gingiva	IV	Ope, S-1, CDDP, DTX, 5FU, RT	PD	0.7	2.3	1 Ag	4W
15	61/M	1	Pharynx	IV	No treatment, inoperable	PD	1.4	1.4	NA	4W
16	49/M	1	Tongue	IV	Ope, S-1, CDDP, DTX, 5FU, RT	PD	1.9	16.3	2 Ag	4W
17	69/F	1	Maxillary gingiva	IV	Ope, BLM, S-1, CDDP, DTX, RT	PD	1.4	1.4	NA	4W
18	56/F	1	Tongue	IV	Ope, S-1, CDDP, DTX, 5FU, RT	CR	37	37	3 Ag	4W
19	71/F	1	Maxillary gingiva	IV	Ope, S-1, RT	SD	2.8	7.7	NA	4W
20	81/F	1	Tongue	IV	Ope, S-1, RT	PD	1	1.8	NA	4W
21	57/M	1	Tongue	IV	Ope, S-1, RT	PD	2.1	2	NA	4W
22	56/F	1	Buccal mucosa	IV	Ope, CDDP, RT	SD	5.1	5.4	2 Ag	4W
23	75/M	1	Mandibular gingiva	IV	Ope, S-1, RT	SD	2.3	3	2 Ag	4W
24	69/M	0	Tongue	IV	S-1, CDDP, DTX, 5FU, RT	SD	2.3	14.3	3 Ag	4W
25	66/M	1	Maxillary gingiva	IV	Ope, S-1, DTX, RT	PD	1.9	11.7	3 Ag	7W
26	67/M	0	Pharynx	IV	S-1, CDDP, DTX, 5FU, RT	PD	1.8	9.5	2 Ag	4W
27	47/M	1	Tongue	IV	Ope, S-1, RT	PD	1	1.6	NA	4W
28	63/F	1	Maxillary gingiva	IV	Ope, S-1, CDDP, DTX, 5FU, RT	SD	15.7	24.8	3 Ag	5W
29	51/M	1	Tongue	IV	Ope, CDDP, DTX, 5FU, RT	PD	1.1	8.3	NA	4W
30	63/M	1	Tongue	IV	CDDP, RT	PD	0.8	0.8	NA	4W
31	65/M	1	Pharynx	IV	S-1, RT	SD	21.8	21.8	2 Ag	4W
32	65/M	1	Tongue	IV	Ope, S-1, CDDP, DTX, 5FU, RT	SD	7	8.1	1 Ag	4W
33	85/F	1	Mandibular gingiva	IV	S-1, RT	PD	1.7	4.6	NA	4W
34	56/M	2	Pharynx	IV	Ope, S-1, CDDP, DTX, 5FU, RT	PD	0.7	1.5	NA	5W
35	76/M	1	Pharynx	IV	Ope, S-1, RT	PD	1.2	1.3	NA	4W
36	36/F	2	Pharynx	IV	S-1, CDDP, DTX, 5FU, RT	PD	1.7	4.8	1 Ag	4W
37	50/M	0	Pharynx	IV	S-1, DTX, RT	SD	11.3	11.3	3 Ag	4W

[a]Stage: staging was carried out according to the TNM classification for HNC (World Health Organization; WHO).
[b]Prior therapy: Ope, surgery; S-1, tegafur, gimeracil, oteracil potassium; CDDP, *cis*diamminedichloroplatinum; DTX, docetaxel; 5FU, fluorouracil; RT, radiotherapy.
[c]Clinical responses were evaluated according to RECIST guidelines.
[d]CTL responses were classified into four subgroups by the number of peptides inducing the positive CTL responses in patients.
[e](x), completion of last treatment; (y), start of vaccination.